Electronic Supplementary Material (ESI) for RSC Advances.

Electronic Supplementary Information

Ionic supramolecular polymerization of water-soluble porphyrins: Balancing ionic attraction and steric repulsion to govern stacking

Chisako Kanzaki, Hiroshi Yoneda, Shota Nomura,
Takato Maeda and Munenori Numata*

Department of Biomolecular Chemistry, Graduate School of Life and Environmental Sciences,
Kyoto Prefectural University, Shimogamo, Sakyo-ku, Kyoto 606-8522, Japan

1. General

UV–Vis spectra were recorded using a JASCO V-670 spectrometer equipped with a thermo controller. Atomic force microscopy (AFM) images were acquired in air using a Shimadzu SPM 9600 microscope (dynamic mode). Each sample was cast on mica and dried for 6 h under reduced pressure prior to observation. Scanning electron microscopy (SEM) was performed using a ZEISS ULTRA55 microscope, operated at an acceleration voltage of 10 kV. An osmium coating was applied using Neoc-Pro (Meiwafosis); the thickness of the coat was adjusted to 5 nm. DLS data were obtained using a Malvern Zetasizer Nano-ZS. Nuclear magnetic resonance (NMR) spectra were recorded using a JEOL Delta V5 400 MHz spectrometer. Infrared (IR) absorption spectrometry was performed using a synchrotron radiation IR beam on BL43IR at SPring-8, Japan. The sample was cast on a CaF_2 substrate and dried under reduced pressure prior to observation. Synchrotron X-ray diffraction (XRD) was performed using a synchrotron radiation X-ray beam on BL40B2 at SPring-8, Japan. The sample was cast on a Kapton film (12.5 μm, Nilaco) and dried under reduced pressure prior to observation. A 30 × 30 cm imaging plate detector was placed 30 cm away from the samples. The diffraction patterns were obtained with an exposure time of 100 s. The wavelength of the incident beam (λ) was 0.071 nm. All reagents and solvents were purchased from Tokyo Chemical Industry, Wako Pure Chemical Industries, and Nacalai Tesque.

2. Sample preparation

Self-assembly in MeOH/aqueous HCl mixed solvent (J-aggregate formation)

A solution of a porphyrin (H_2TPPS_2-NHCO-EG_x) in MeOH (100 μM) was prepared. Each of the porphyrin derivatives existed in a monomeric state under these conditions. The solution was mixed with aqueous HCl (pH 3) in a vial. The final concentration was adjusted to 25 μM; the final solvent composition was MeOH/aqueous HCl, 25/75 (v/v).

Sample preparation for XRD measurements

A solution of a porphyrin (H_2TPPS_2-NHCO-EG_x) in MeOH (500 μM) was mixed with aqueous HCl (pH 2). The final concentration was 125 μM; the final solvent composition was MeOH/aqueous HCl, 25/75 (v/v). The formed precipitate was subjected to XRD measurements.

Self-assembly in MeOH/pure water mixed solvent (H-aggregate formation)

A solution of a porphyrin (H_2TPPS_2-NHCO-EG_x) in MeOH (100 μM) was mixed with ultrapure water. The final concentration was 25 μM; the final solvent composition was

MeOH/water 25/75, (v/v). To measure the spectral changes with respect to solvent composition, the final MeOH/water composition was varied from 100:0 to 5:95 (v/v) while retaining a constant concentration (25 μM).

3. Syntheses of H_2TPPS_2-NHCO-EG$_x$ (x = 2, 4, 6, 8, 18) porphyrin derivatives

The H_2TPPS_2-NHCO-EG$_x$ (x = 2, 4, 6, 8, 18) porphyrin derivatives were synthesized according to Scheme S1.

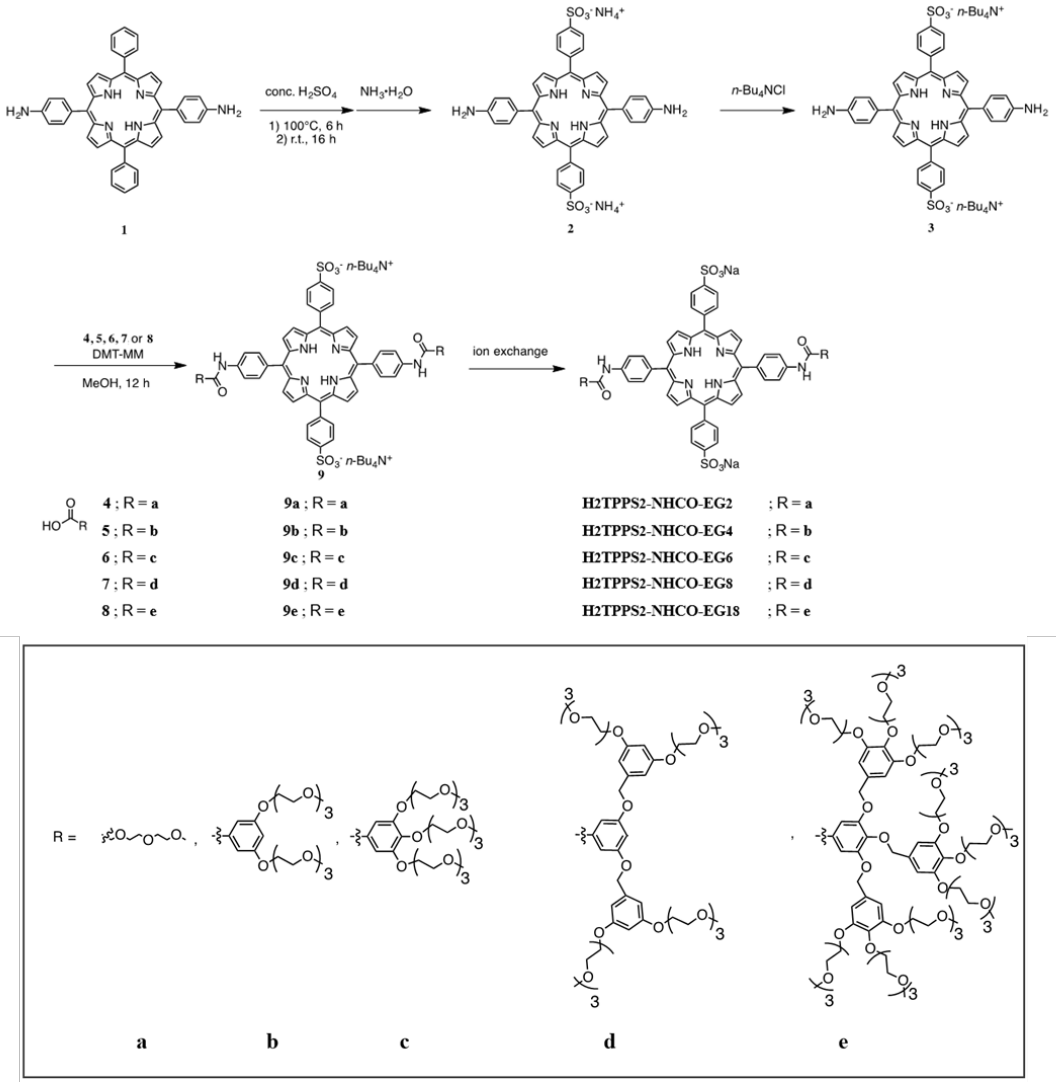

Scheme S1. Syntheses of **H_2TPPS_2-NHCO-EG$_x$** (x = 2, 4, 6, 8, 18) porphyrin derivatives.

Compound 1:

Compound **1** was synthesized according to the method reported by T. Lin and co-workers.[1]

Compound 2:

Compound **2** was synthesized using a method similar to that reported by A. Arlegui and co-workers.[2] Compound **1** (230 mg, 0.357 mmol, 1.0 eq.) was dissolved in conc. H_2SO_4 (15 mL) and then the mixture was stirred at 100 °C for 6 h. The dark-green solution was then stirred for 16 h at room temperature and poured into cold water (20 mL). The mixture was neutralized with ammonium hydroxide (28%). The dark-purple solution was used in the next step without further purification.

Compound 3:

An aqueous solution of compound **2** (230 mg, 0.357 mmol, 1.0 eq.) was poured into aqueous tetrabutylammonium chloride (TBA-Cl, 298 mg, 1.07 mmol, 3.0 eq., 10 mL) and then the aqueous phase was extracted with CH_2Cl_2. The combined organic phases were dried (anhydrous Na_2SO_4) to yield a purple solid (432 mg, including excess TBA-Cl, 80%).

^{1}H NMR (400 MHz, DMSO-d_6): δ 8.97–8.73 (m, 8H, β-pyrrole), 8.19 (d, J = 7.9 Hz, 4H, ArH), 8.07 (d, J = 7.9 Hz, 4H, ArH), 7.88 (d, J = 8.6 Hz, 4H, ArH), 7.03 (d, J = 7.9 Hz, 4H, ArH), 5.62 (s, 4H, NH_2), 3.10 (t, J = 8.3 Hz, 17H), 1.54–1.39 (m, 17H), 1.29–1.20 (m, 17H), 0.90–0.77 (m, 26H), –2.80 (s, 2H, pyrrole NH). ^{13}C NMR (100 MHz, DMSO-d_6) δ = 148.7, 147.9, 141.5, 135.5, 133.7, 131.5, 128.3, 124.2, 121.3, 119.1, 112.6, 57.4, 23.0, 19.2, 13.5.

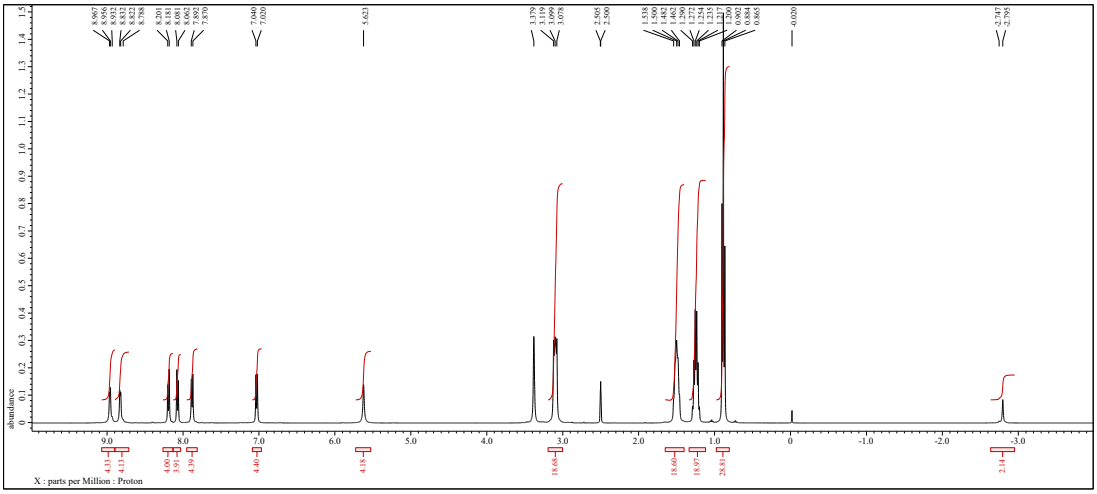

Fig. S1. ^{1}H NMR spectrum of **Compound 3** in DMSO-d_6 at r.t.

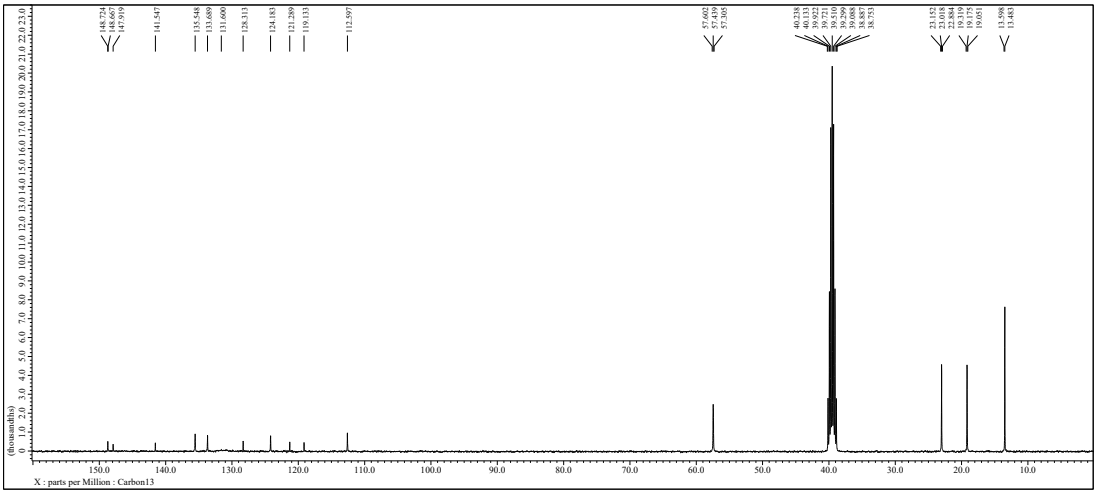

Fig. S2. ^{13}C NMR spectrum of **Compound 3** in DMSO-d_6 at r.t.

Compound 4:

[2-(2-Methoxyethoxy)ethoxy]acetic acid (**compound 4**) was purchased from Tokyo Chemical Industry.

Compounds 5 and 6:

Compounds **5** and **6** were synthesized using methods similar to those reported by V. Percec and co-workers.[3]

Compounds 7 and 8:

Compounds **7** and **8** were synthesized using methods similar to those reported by A. Bertin and co-workers.[4]

Compound 9a:

Compound **9a** was synthesized using a method similar to that reported by H. Kitagishi and co-workers.[5] Compound **3** (80 mg, 0.062 mmol, 1.0 eq.), [2-(2-methoxyethoxy)ethoxy]acetic acid (55 mg, 0.31 mmol, 5.0 eq.), and 4-(4,6-dimethoxy-1,3,5-triazin-2-yl)-4-methylmorpholinium chloride (DMT-MM; 86 mg, 0.31 mmol, 5.0 eq.) were dissolved in MeOH (5 mL) and then the mixture was stirred at r.t. for 12 h. The mixture was poured into aqueous $NaHCO_3$ (sat.) (10 mL) and extracted with CH_2Cl_2. The combined organic phases were dried (anhydrous Na_2SO_4). The residue was purified through column chromatography (CH_2Cl_2/MeOH/triethylamine, from 90/10/1 to 80/20/1) to yield a dark-purple solid (44 mg, 44%).

^{1}H NMR (400 MHz, $CDCl_3$, TMS, r.t.): δ = 9.19 (s, 2H, amide NH), 8.89–8.83 (m, 8H, β-pyrrole), 8.30 (d, *J* = 7.9 Hz, 4H), 8.23 (d, *J* = 7.9 Hz, 4H), 8.17 (d, *J* = 8.6 Hz, 4H), 8.03 (d, *J* = 7.9 Hz, 4H), 4.28 (s, 4H, CH_2), 3.92–3.90 (m, 4H, OCH_2), 3.92–3.90 (m, 4H, OCH_2), 3.86–3.80 (m, 4H, OCH_2), 3.70–3.66 (m, 4H, OCH_2), 3.42 (s, 6H, OCH_3), 3.24–3.17 (m, 16H, TBA-CH_2), 1.47–1.40 (m, 24H, TBA-CH_3), –2.83 (s, 2H, pyrrole NH).

Compound 9b:

Compound **3** (130 mg, 0.086 mmol, 1.0 eq.), Compound **5** (153 mg, 0.34 mmol, 4.0 eq.), and DMT-MM (119 mg, 0.43 mmol, 5.0 eq.) were dissolved in MeOH (5 mL) and then the mixture was stirred at r.t. for 22 h. The mixture was poured into aqueous $NaHCO_3$ (sat.) (10 mL) and extracted with CH_2Cl_2. The combined organic phases were dried (anhydrous Na_2SO_4). The residue was purified through column chromatography (CH_2Cl_2/MeOH/triethylamine, from 90/10/1 to 85/15/1) to yield a dark-purple solid (67 mg, 33%).

^{1}H NMR (400 MHz, $CDCl_3$, TMS, r.t.): δ = 8.91–8.85 (m, 8H, β-pyrrole), 8.58 (s, 2H, amide NH), 8.30–8.19 (m, 12H, ArH), 8.08 (d, *J* = 7.9 Hz, 4H, ArH), 6.74 (s, 2H, ArH), 4.25 (t, *J* = 4.3 Hz, 8H, OCH_2), 3.93–3.90 (m, 8H, OCH_2), 3.78–3.77 (m, 8H, OCH_2), 3.73–3.66 (m, 16H, OCH_2), 3.58–3.56 (m, 8H, OCH_2), 3.39 (s, 12H, OCH_3), 3.18 (q, *J* = 7.3 Hz, 26H, TBA-CH_2), 1.47–1.41 (m, 40H, TBA-CH_3), –2.83 (s, 2H, pyrrole NH).

Compound 9c:

Compound **3** (80 mg, 0.062 mmol, 1.0 eq.), Compound **6** (189 mg, 0.31 mmol, 5.0 eq.), and DMT-MM (86 mg, 0.31 mmol, 5.0 eq.) were dissolved in MeOH (10 mL) and then the mixture was stirred at r.t. for 16 h. The mixture was poured into aqueous $NaHCO_3$ (sat.) (20 mL) and extracted with CH_2Cl_2. The combined organic phases were dried (anhydrous Na_2SO_4). The residue was purified through column chromatography (CH_2Cl_2/MeOH/triethylamine, from 95/5/1 to 90/10/1) to yield a dark-purple solid (84 mg, 55%).

^{1}H NMR (400 MHz, $CDCl_3$, TMS, r.t.): δ = 9.04 (s, 2H, amide NH), 8.90 (d, *J* = 4.8 Hz, 4H, β-pyrrole), 8.83 (d, *J* = 4.8 Hz, 4H, ArH), 8.29 (d, *J* = 8.0 Hz, 4H, ArH), 8.21 (d, *J* = 8.0 Hz, 4H, ArH), 8.19–8.12 (m, 8H, β-pyrrole), 7.45 (s, 4H, ArH), 4.35 (t, *J* = 4.4 Hz, 8H, OCH_2), 4.29 (t, *J* = 4.4 Hz, 4H, OCH_2), 3.91 (t, *J* = 4.4 Hz, 8H, OCH_2), 3.85 (t, *J* = 4.4 Hz, 4H, OCH_2), 3.79–3.62 (m, 36H, OCH_2), 3.58–3.52 (m, 12H, OCH_2), 3.39 (s, 6H, OCH_3), 3.36 (s, 12H, OCH_3), 3.24–3.17 (m, 16H, TBA-CH_2), 1.47–1.40 (m, 24H, TBA-CH_3), –2.84 (s, 2H, pyrrole NH).

Compound 9d:

Compound **3** (35 mg, 0.023 mmol, 1.0 eq.), Compound **7** (68 mg, 0.069 mmol, 3.0 eq.), and DMT-MM (32 mg, 0.12 mmol, 5.0 eq.) were dissolved in MeOH (5 mL) and then the mixture was stirred at r.t. for 18 h. The mixture was poured into aqueous $NaHCO_3$ (sat.) (10 mL) and extracted with CH_2Cl_2. The combined organic phases were dried (anhydrous Na_2SO_4). The residue was purified through column chromatography (CH_2Cl_2/MeOH/triethylamine, from 95/5/1 to 80/20/1) to yield a dark-purple solid (50 mg, 50%).

^{1}H NMR (400 MHz, $CDCl_3$, TMS, r.t.) δ = 8.87 (d, *J* = 4.6 Hz, 8H, β-pyrrole), 8.47 (s, 2H, amide NH), 8.30 (d, *J* = 7.9 Hz, 3H, ArH), 8.22 (d, *J* = 8.6 Hz, 8H, ArH), 8.09 (d, *J* = 8.6 Hz, 4H, ArH), 7.28 (s, 4H, ArH), 6.82 (s, 2H, ArH), 6.66 (s, 8H, ArH), 6.48 (s, 4H, ArH), 5.10 (s, 8H, CH_2), 4.14 (t, *J* = 4.6 Hz, 16H, OCH_2), 3.85 (t, *J* = 4.6 Hz, 16H, OCH_2), 3.74–3,72 (m, 16H, OCH_2), 3.68–3.63 (m, 32H, OCH_2), 3.54–3.51 (m, 16H, OCH_2), 3.35 (s, 24H, OCH_3), 3.21–3.16 (m, 28H, TBA-CH_2), 1.49–1.42 (m, 42H, TBA-CH_3), –2.83 (s, 2H, pyrrole NH).

Compound 9e:

Compound **3** (22 mg, 0.015 mmol, 1.0 eq.), Compound **8** (80 mg, 0.045 mmol, 3.0 eq.), and DMT-MM (21 mg, 0.075 mmol, 5.0 eq.) were dissolved in MeOH (5 mL) and then the mixture was stirred at r.t. for 18 h. The mixture was poured into aqueous $NaHCO_3$ (sat.) (10 mL) and extracted with CH_2Cl_2. The combined organic phases were dried (anhydrous Na_2SO_4). The residue was purified through column chromatography (CH_2Cl_2/MeOH/triethylamine, from 95/5/1 to 90/10/1) to yield a dark-purple solid (55 mg, 40%).

^{1}H NMR (400 MHz, $CDCl_3$, TMS, r.t.) δ = 8.87–8.81 (m, 8H, β-pyrrole), 8.29 (d, *J* = 7.9 Hz, 4H, ArH), 8.19 (d, *J* = 7.9 Hz, 8H, ArH), 8.14 (d, *J* = 8.6 Hz, 4H, ArH), 7.51 (s, 4H, ArH), 6.75 (s, 8H, ArH), 6.67 (s, 4H, ArH), 5.19 (s, 8H, CH_2), 5.09 (s, 4H, CH_2), 4.15–3.97 (m, 36H, OCH_2), 3.81–3.75 (m, 36H, OCH_2), 3.71–3.57 (m, 108H, OCH_2), 3.55–3.46 (m, 36H, OCH_2), 3.38–3.30 (m, 54H, OCH_3), 3.17–3.06 (m, 136H, TBA-CH_2), 1.44–1.36 (m, 204H, TBA-CH_3), –2.86 (s, 2H, pyrrole NH).

H_2TPPS_2-NHCO-EG_2:

Compound **9a** was dissolved in distilled water/MeOH (1/1, v/v) and then the solution was passed through an ion exchange column (Amberlite® ion exchange resin; Na-form). After washing the aqueous solution with hexane and CH_2Cl_2, evaporation of the solvent under reduced pressure to yield a dark-purple solid (20 mg, 63%).

^{1}H NMR (400 MHz, DMSO-d_6, r.t.) δ = 10.17 (s, 2H, amide NH), 8.92–9.02 (m, 8H, β-pyrrole), 8.27–8.21 (m, 8H, ArH), 8.18 (d, J = 8.6 Hz, 4H, ArH), 8.12 (d, J = 8.6 Hz, 4H, ArH), 4.31 (s, 4H, CH_2), 3.84 (q, J = 3.1 Hz, 4H, OCH_2), 3.74 (q, J = 3.1 Hz, 4H, OCH_2), 3.65–3.69 (m, 4H, OCH_2), 3.58–3.55 (m, 4H, OCH_2), 3.33 (s, 6H, OCH_3), –2.84 (s, 2H, pyrrole NH). ^{13}C NMR (100 MHz, DMSO-d_6, r.t.) δ = 168.9, 147.8, 141.5, 138.5, 136.4, 134.7, 133.8, 131.4, 124.3, 129.9, 119.7, 118.1, 71.3, 70.5, 70.4, 69.8, 69.7, 58.2. MS (MALDI-TOF, negative mode, α-CHCA) m/z 1123.4 (calcd. for $[M - 2Na + H]^-$, 1123.3).

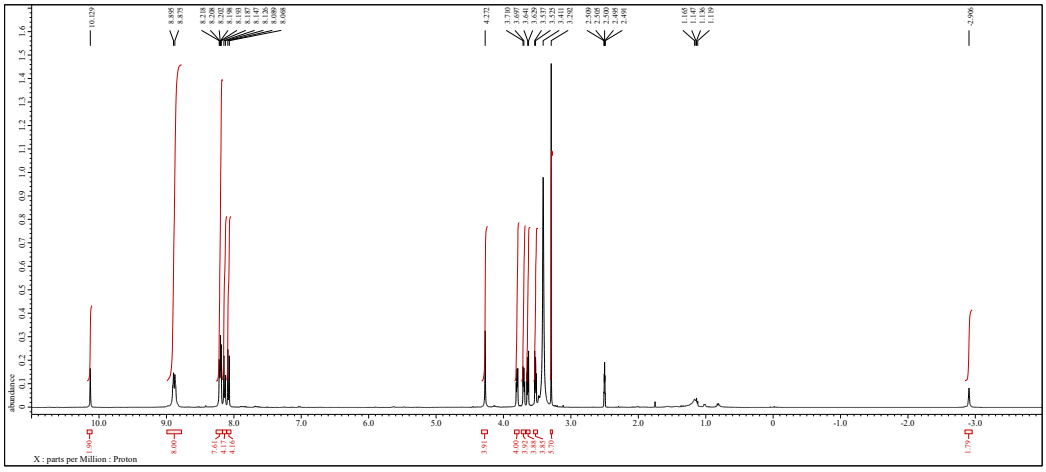

Fig. S3. ^{1}H NMR spectrum of **H_2TPPS$_2$-NHCO-EG$_2$** in DMSO-d_6 at r.t.

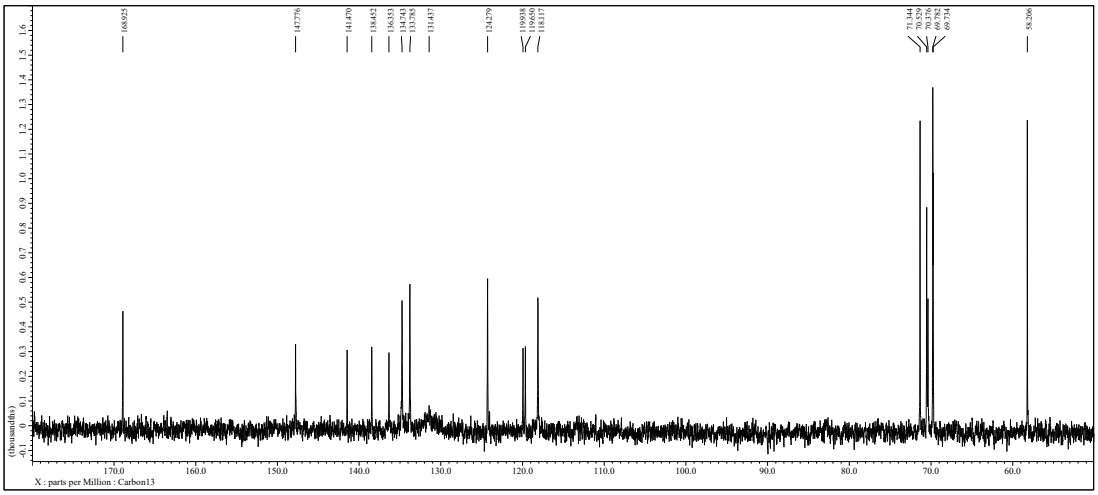

Fig. S4. ^{13}C NMR spectrum of **H_2TPPS$_2$-NHCO-EG$_2$** in DMSO-d_6 at r.t.

H_2TPPS$_2$-NHCO-EG$_4$:

Compound **9b** was dissolved in distilled water/MeOH (9/1, v/v) and then the solution was passed through an ion exchange column (Amberlite® ion exchange resin; Na-form).

After washing the aqueous solution with hexane and CH_2Cl_2, evaporation of the solvent under reduced pressure to yield a dark-purple solid (43 mg, 91%).
^{1}H NMR (400 MHz, DMSO-d_6, r.t.) δ = 10.67 (s, 2H, amide NH), 9.09–8.89 (m, 8H, β-pyrrole), 8.33–8.21 (m, 12H, ArH), 8.09 (d, J = 7.9 Hz, 4H, ArH), 7.30 (s, 4H, ArH), 6.87 (s, 2H, ArH), 4.28–4.18 (m, 8H, OCH_2), 3.85–3.76 (m, 8H, OCH_2), 3.65–3.59 (m, 8H, OCH_2), 3.57–3.50 (m, 16H, OCH_2), 3.47–3.42 (m, 8H, OCH_2), 3.25 (s, 12H, OCH_3), –2.88 (s, 2H, pyrrole NH). ^{13}C NMR (100 MHz, DMSO-d_6, r.t.) δ = 165.5, 159.7, 147.8, 141.5, 139.2, 137.1, 136.4, 134.7, 133.8, 131.7, 124.3, 120.0, 119.7, 118.8, 106.5, 104.2, 71.3, 70.0, 69.9, 69.7, 69.0, 67.6, 58.1. MS (MALDI-TOF, negative mode, α-CHCA) m/z 1659.1 (calcd. for $[M - 2Na + H]^-$, 1659.6).

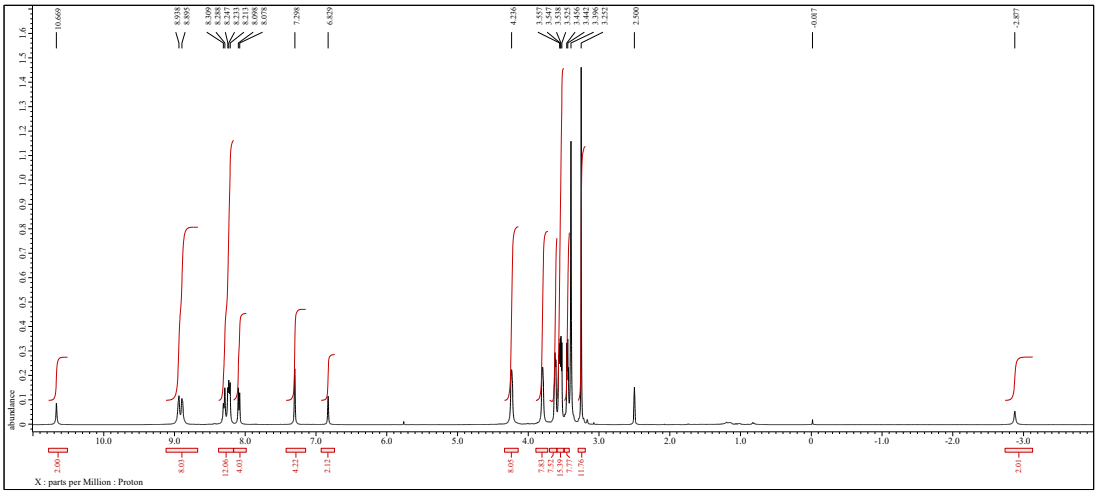

Fig. S5. ^{1}H NMR spectrum of **H_2TPPS$_2$-NHCO-EG$_4$** in DMSO-d_6 at r.t.

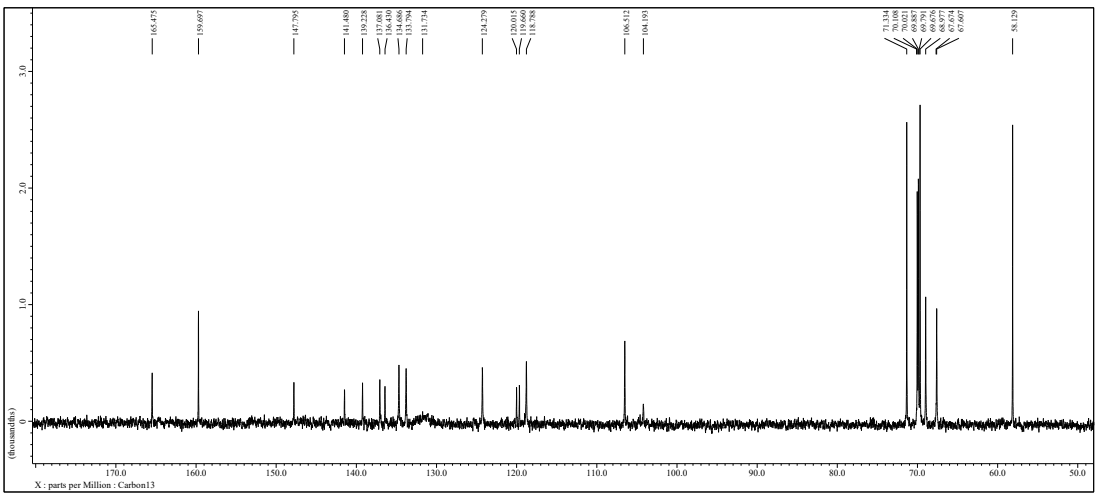

Fig. S6. ^{13}C NMR spectrum of **H_2TPPS$_2$-NHCO-EG$_4$** in DMSO-d_6 at r.t.

H_2TPPS_2-NHCO-EG_6:

Compound **9c** was dissolved in distilled water/MeOH (1/1, v/v) and then the solution was passed through an ion exchange column (Amberlite® ion exchange resin; Na-form). After washing the aqueous solution with hexane and CH_2Cl_2, evaporation of the solvent under reduced pressure to yield a dark-purple solid (67 mg, 98%).

^{1}H NMR (400 MHz, DMSO-d_6, r.t.) δ = 10.61 (s, 2H, amide NH), 9.11–8.90 (m, 8H, β-pyrrole), 8.41–8.21 (m, 12H, ArH), 8.09 (d, J = 7.9 Hz, 4H, ArH), 7.46 (s, 4H, ArH), 4.35–4.24 (m, 8H, OCH_2), 4.15 (t, J = 4.6 Hz, 4H, OCH_2), 3.87–3.78 (m, 8H, OCH_2), 3.73–3.69 (m, 4H, OCH_2), 3.64 (t, J = 4.6 Hz, 8H), 3.61–3.49 (m, 28H, OCH_2), 3.48–3.43 (m, 12H, OCH_2), 3.28–3.21 (m, 18H, OCH_3), –2.81 (s, 2H, pyrrole NH). ^{13}C NMR (100 MHz, DMSO-d_6, r.t.) δ = 165.4, 152.1, 147.8, 141.5, 140.5, 139.3, 136.4, 134.7, 133.8, 131.3, 130.0, 124.3, 120.0, 119.7, 118.9, 107.1, 72.0, 71.4, 70.1, 70.0, 69.8, 69.7, 69.1, 68.6, 58.1. MS (MALDI-TOF, negative mode, α-CHCA) m/z 1983.7 (calcd. for [M – 2Na + H]$^-$, 1983.7).

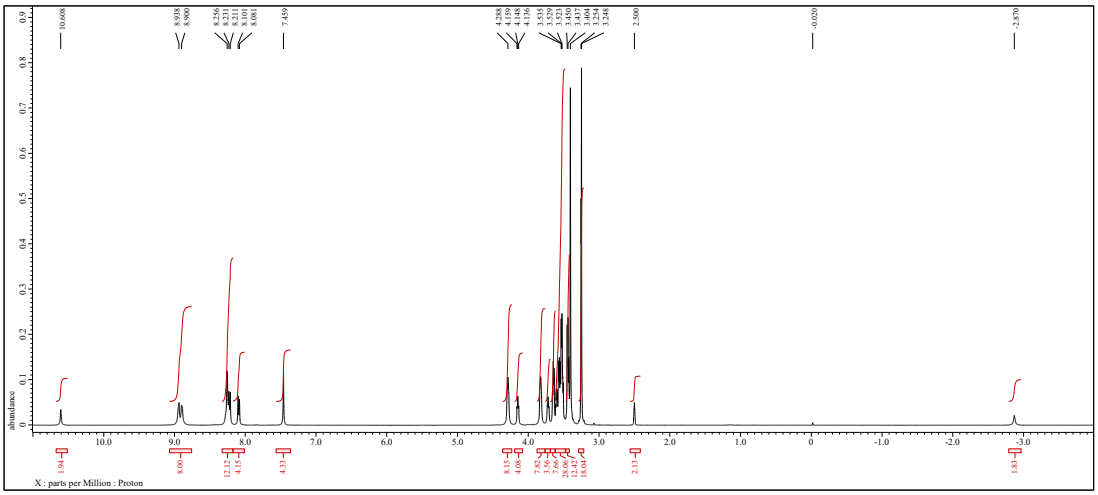

Fig. S7. ^{1}H NMR spectrum of **H_2TPPS_2-NHCO-EG_6** in DMSO-d_6 at r.t.

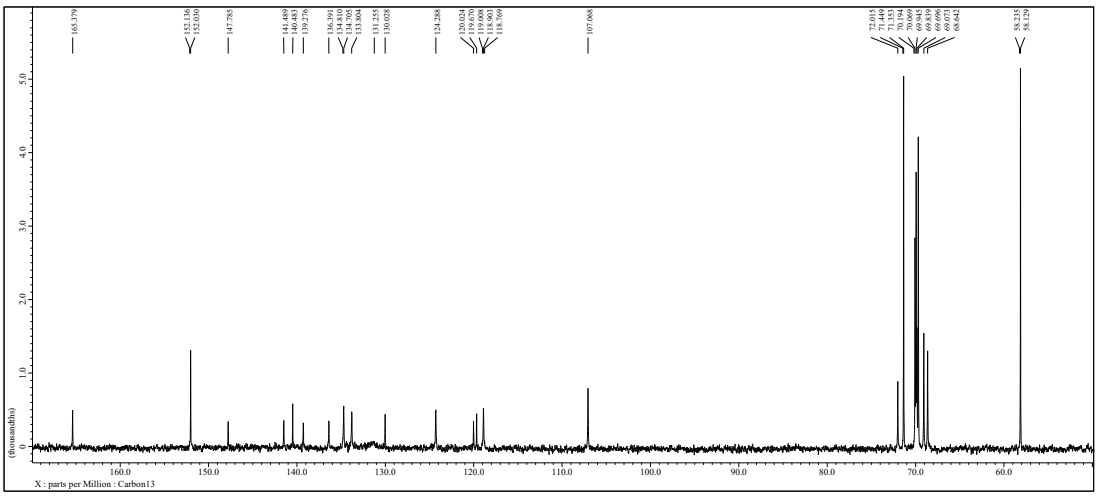

Fig. S8. ^{13}C NMR spectrum of **H_2TPPS$_2$-NHCO-EG$_6$** in DMSO-d_6 at r.t.

H_2TPPS$_2$-NHCO-EG$_8$:

Compound **9d** was dissolved in distilled water/MeOH (9/1, v/v) and then the solution was passed through an ion exchange column (Amberlite® ion exchange resin; Na-form). After washing the aqueous solution with hexane and CH_2Cl_2, evaporation of the solvent under reduced pressure to yield a dark-purple solid (40 mg, almost quantitative yield).

^{1}H NMR (400 MHz, DMSO-d_6) δ = 10.67 (s, 2H, amide NH), 8.93–8.88 (m, 8H, β-pyrrole), 8.27–8.20 (m, 12H, ArH), 8.08 (d, J = 7.9 Hz, 4H, ArH), 7.38 (s, 4H, ArH), 6.97 (s, 2H, ArH), 6.70 (s, 8H, ArH), 6.52 (s, 4H, ArH), 5.19 (s, 8H, CH_2), 4.11 (t, J = 4.3 Hz, 16H, OCH_2), 3.74 (t, J = 4.3 Hz, 16H, OCH_2), 3.59–3.57 (m, 16H, OCH_2), 3.53–3.49 (m, 32H, OCH_2), 3.44–3.41 (m, 16H, OCH_2), 3.21 (s, 24H, OCH_3), –2.88 (s, 2H, pyrrole NH).

^{13}C NMR (100 MHz, DMSO-d_6) δ 165.4, 169.8, 159.5, 147.8, 141.5, 141.9, 139.2, 137.2, 136.5, 134.7, 133.8, 131.8, 124.3, 120.0, 119.7, 118.8, 107.0, 106.2, 100.5, 71.8, 70.5, 70.3, 70.1, 70.0, 69.4, 67.8, 58.6. MS (MALDI-TOF, negative mode, α-CHCA) m/z 2732.0 (calcd. for $[M - 2Na + H]^-$, 2732.1).

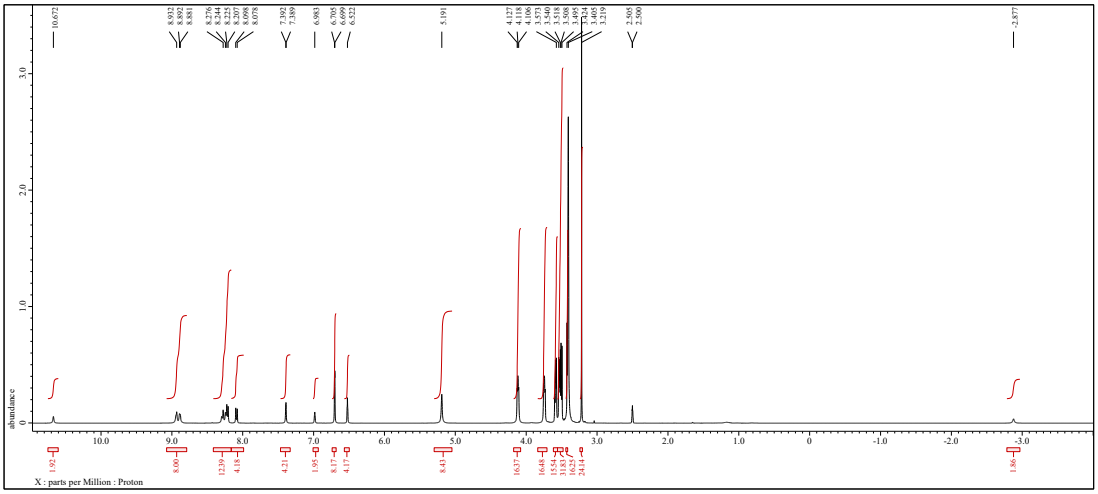

Fig. S9. ^{1}H NMR spectrum of **H_2TPPS_2-NHCO-EG_8** in DMSO-d_6 at r.t.

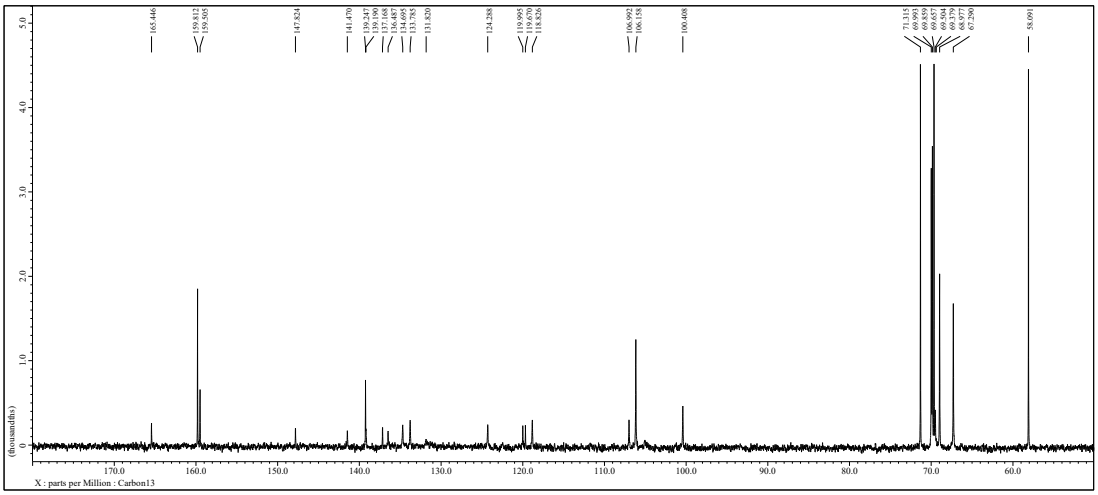

Fig. S10. ^{13}C NMR spectrum of **H_2TPPS_2-NHCO-EG_8** in DMSO-d_6 at r.t.

H_2TPPS_2-NHCO-EG_{18}:

Compound **9e** was dissolved in distilled water and then the solution was passed through an ion exchange column (Amberlite® ion exchange resin; Na-form). After washing the aqueous solution with hexane and CH_2Cl_2, evaporation of the solvent under reduced pressure to yield a dark-purple solid (41 mg, almost quantitative yield).

^{1}H NMR (400 MHz, DMSO-d_6) δ = 10.64 (s, 2H, amide NH), 8.94–8.88 (m, 8H, β-pyrrole), 8.26–8.20 (m, 12H, ArH), 8.08 (d, J = 7.9 Hz, 4H, ArH), 7.64 (s, 4H, ArH), 6.89

(s, 8H, ArH), 6.76 (s, 4H, ArH), 5.25 (s, 8H, CH_2), 5.09 (s, 4H, CH_2), 4.06–3.93 (m, 36H, OCH_2), 3.73–3.69 (m, 36H, OCH_2), 3.59–3.47 (m, 108H, OCH_2), 3.45–3.37 (m, 36H, OCH_2), 3.25 (s, 6H, OCH_3), 3.22 (s, 24H, OCH_3), 3.19 (s, 24H, OCH_3), –2.88 (s, 2H, pyrrole NH). ^{13}C NMR (100 MHz, DMSO-d_6) δ 165.2, 152.3, 152.1, 152.0, 147.8, 141.4, 140.3, 137.1, 137.0, 134.7, 133.7, 133.2, 132.3, 130.3, 124.3, 120.0, 119.7, 118.9, 107.7, 106.6, 106.3, 74.7, 72.4, 71.8, 71.8, 71.2, 70.5, 70.4, 70.3, 70.1, 69.5, 68.8, 68.7, 58.6, 58.5. MS (MALDI-TOF, negative mode, α-CHCA) *m*/*z* 4564.7 (calcd. for [M – 2Na + 2H]$^-$, 4565.1).

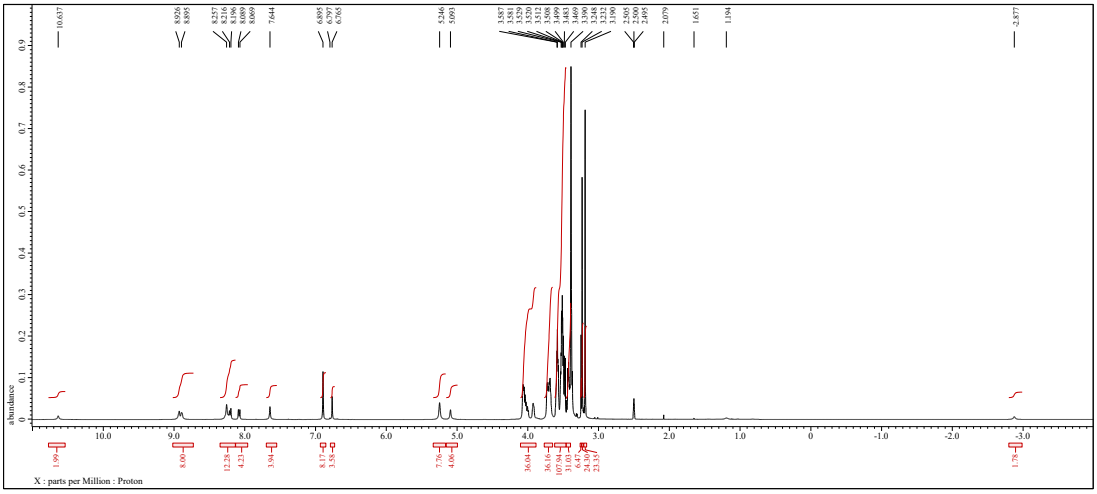

Fig. S11. ^{1}H NMR spectrum of **H_2TPPS$_2$-NHCO-EG$_{18}$** in DMSO-d_6 at r.t.

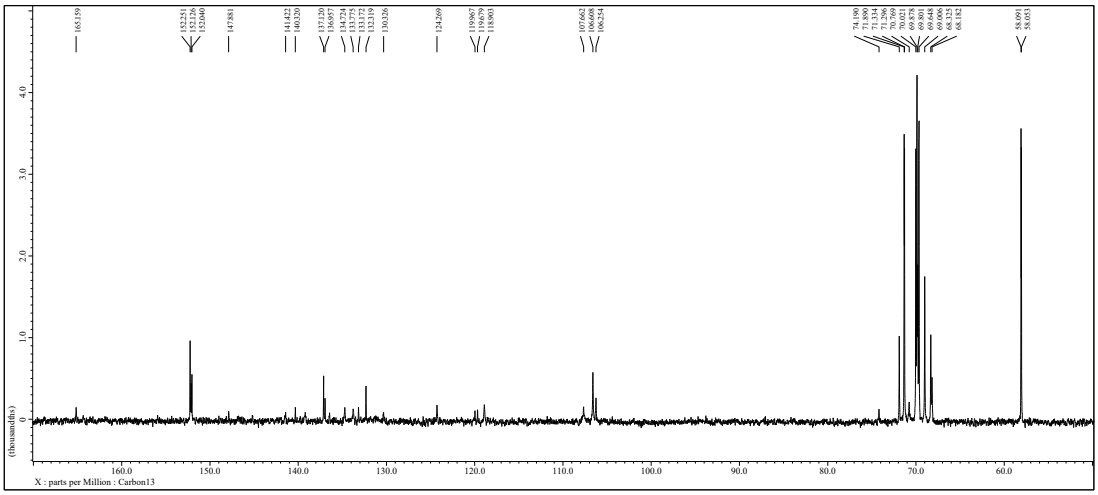

Fig. S12. ^{13}C NMR spectrum of **H_2TPPS$_2$-NHCO-EG$_{18}$** in DMSO-d_6 at r.t.

4. Synthesis of H_2TPPS_2-O-EG_2

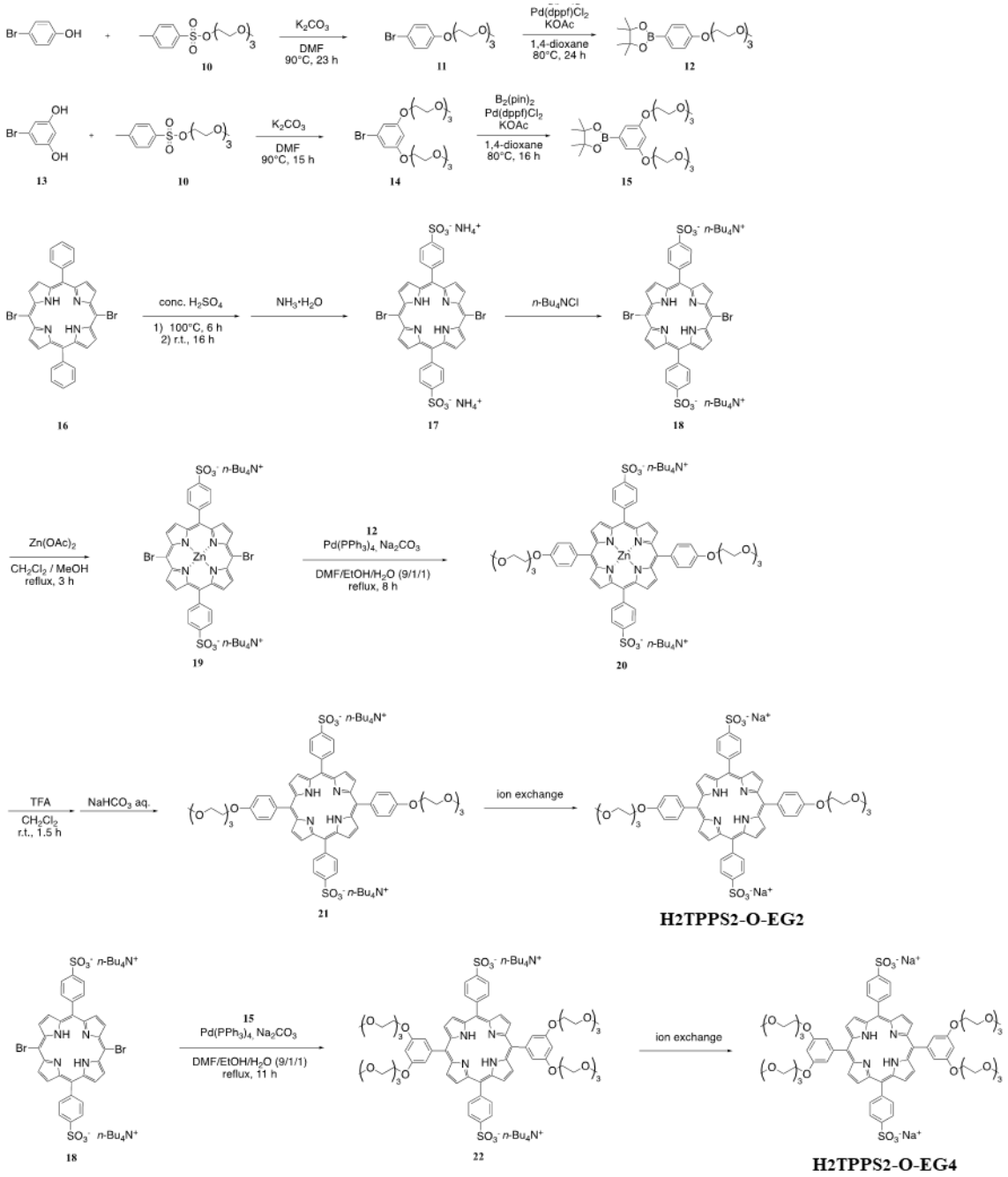

Scheme S2. Syntheses of **H_2TPPS_2-O-EG_x** (x = 2, 4) porphyrin derivatives.

Compound 10:

Compound **10** was synthesized using methods similar to those reported by V. Percec and co-workers.[3]

Compound 11:

Compound **10** (2.20 g, 6.93 mmol, 1.2 eq.), 4-bromophenol (1.00 g, 5.77 mmol, 1.0 eq.) and K_2CO_3 (8.00 g, 57.7 mmol, 10.0 eq.) were dissolved in *N*,*N*-dimethylformamide (DMF, 20 mL) and then the mixture was stirred at 90 °C for 23 h under a N_2 atmosphere. The mixture was poured into aqueous HCl (1.0 M, 20 mL) and extracted with EtOAc. The combined organic phases were dried (anhydrous $MgSO_4$). The residue was purified through column chromatography (hexane/EtOAc, 1/1) to yield a clear oil (1.0 g, 99%).

^{1}H NMR (400 MHz, $CDCl_3$, TMS, r.t.) δ = 7.39–7.34 (m, 2H, ArH), 6.82–6.78 (m, 2H, ArH), 4.11–4.08 (m, 2H, OCH_2), 3.87–3.83 (m, 2H, OCH_2), 3.75–3.72 (m, 2H, OCH_2), 3.69–3.64 (m, 4H, OCH_2), 3.56–3.53 (m, 2H, OCH_2), 3.38 (s, 3H, OCH_3).

Compound 12:

Compound **11** (200 mg, 0.63 mmol, 1.0 eq.), bis(pinacolato)diboron (254 mg, 1.00 mmol, 1.6 eq.), Pd(dppf)Cl_2 (10 mg, 5%), and KOAc (185 mg, 1.89 mmol, 3.0 eq.) were dissolved in anhydrous 1,4-dioxane (20 mL) and then the mixture was stirred at 80 °C for 24 h under a N_2 atmosphere. The mixture was poured into water (10 mL) and extracted with EtOAc. The combined organic phases were dried (anhydrous $MgSO_4$). The residue was purified through column chromatography (hexane/EtOAc, 1/9) to yield a clear oil (93.1 mg, 40.4%).

^{1}H NMR (400 MHz, $CDCl_3$, TMS, r.t.) δ = 7.73 (d, *J* = 8.0 Hz, 2H, ArH), 6.90 (d, *J* = 8.0, 2H, ArH), 4.16 (t, *J* = 5.0 Hz, 2H, OCH_2), 3.86 (t, *J* = 5.0 Hz, 2H, OCH_2), 3.73–3.76 (m, 2H, OCH_2), 3.64–3.70 (m, 4H, OCH_2), 3.56–3.54 (m, 2H, OCH_2), 3.38 (s, 3H, OCH_3), 1.35 (s, 12H, CH_3).

Compound 13:

Compound **13** was synthesized using methods similar to those reported by V. R. L. J. Bloemendal and co-workers.[6]

Compound 14:

Compound **10** (236 mg, 0.74 mmol, 2.0 eq.), Compound **13** (70 mg, 0.37 mmol, 1.0 eq.) and K_2CO_3 (219 mg, 0.37 mmol, 10.0 eq.) were dissolved in *N*,*N*-dimethylformamide (DMF, 10 mL) and then the mixture was stirred at 90 °C for 15 h under a N_2 atmosphere.

The mixture was poured into aqueous HCl (1.0 M, 20 mL) and extracted with EtOAc. The combined organic phases were dried (anhydrous $MgSO_4$). The residue was purified through column chromatography (hexane/EtOAc, 1/1) to yield a clear oil (164 mg, 92%). ^{1}H NMR (400 MHz, $CDCl_3$, TMS, r.t.) δ = 6.67 (d, *J* = 2.3 Hz, 2H, ArH), 6.42-6.40 (m, 1H, ArH), 4.08–4.02 (m, 4H, OCH_2), 3.88–3.79 (m, 4H, OCH_2), 3.75–3.71 (s, 4H, OCH_2), 3.69–3.64 (m, 8H, OCH_2), 3.56–3.53 (m, 4H, OCH_2), 3.38 (s, 6H, OCH_3).

Compound 15:

Compound **14** (163 mg, 0.34 mmol, 1.0 eq.), bis(pinacolato)diboron (138 mg, 0.54 mmol, 1.6 eq.), Pd(dppf)Cl_2 (8.0 mg, 5%), and KOAc (100 mg, 1.02 mmol, 3.0 eq.) were dissolved in anhydrous 1,4-dioxane (20 mL) and then the mixture was stirred at 80 °C for 16 h under a N_2 atmosphere. The mixture was poured into water (10 mL) and extracted with EtOAc. The combined organic phases were dried (anhydrous $MgSO_4$). The residue was purified through column chromatography (hexane/EtOAc, 1/9) to yield a clear oil (65 mg, 36%).

^{1}H NMR (400 MHz, $CDCl_3$, TMS, r.t.) δ = 6.95 (d, *J* = 2.3 Hz, 2H, ArH), 6.61–6.58 (m, 1H, ArH), 4.14 (t, *J* = 4.8 Hz, 4H, OCH_2), 3.88–3.81 (m, 4H, OCH_2), 3.75–3.72 (m, 4H, OCH_2), 3.69–3.65 (m, 4H, OCH_2), 3.57–3.53 (m, 4H, OCH_2), 3.38 (s, 6H, OCH_3), 1.37–1.33 (s, 12H, CH_3).

Compound 16:

Compound **15** was synthesized using methods similar to those reported by X. Jiang and co-workers.[7]

Compound 17:

Compound **16** was synthesized using a method similar to that reported by A. Arlegui and co-workers.[2] Compound **15** (40.0 mg, 0.065 mmol, 1.0 eq.) was dissolved in conc. H_2SO_4 (15 mL) and then the mixture was stirred at 100 °C for 6 h. The dark-green solution was then stirred for 16 h at room temperature and poured into cold water (20 mL). The mixture was neutralized with ammonium hydroxide (28%). The dark-purple solution was used in the next step without further purification.

Compound 18:

An aqueous solution of compound **16** (46.6 mg, 0.0630 mmol, 1.0 eq.) was poured into aqueous TBA-Cl (39.5 mg, 0.140 mmol, 2.2 eq., 10 mL) and then the aqueous mixture was extracted with CH_2Cl_2. The combined organic phases were dried (anhydrous Na_2SO_4)

to yield a purple solid (76.5 mg, including excess TBA-Cl, 94%).
^{1}H NMR (400 MHz, $CDCl_3$, TMS, r.t.) δ = 9.60 (d, *J* = 4.9 Hz, 4H, β-pyrrole), 8.84–8.87 (m, 4H, β-pyrrole), 8.35 (d, *J* = 6.0 Hz, 4H, ArH), 8.12 (d, *J* = 6.1 Hz, 4H, ArH), 3.31–3.40 (m, 43H, TBA-CH_2), 1.62–1.70 (m, 44H, TBA-CH_2), 1.48–1.39 (m, 45H, TBA-CH_2), 0.97–1.05 (m, 68H, TBA-CH_3), –2.78 (s, 2H, pyrrole NH).

Compound 19:
Compound **18** (76.5 mg, 0.0610 mmol, 1.0 eq.) and $Zn(OAc)_2$ (66.4 mg, 0.302 mmol, 1.0 eq.) in MeOH (5 mL) were dissolved in CH_2Cl_2 (30 mL) and then the mixture was stirred at 65 °C for 3 h. The mixture was poured into aqueous $NaHCO_3$ (sat.) (20 mL) and extracted with CH_2Cl_2. The combined organic phases were dried (anhydrous Na_2SO_4) to yield a dark-green solid (16.9 mg, 21%).
^{1}H NMR (400 MHz, $CDCl_3$, TMS, r.t.) δ = 9.66 (s, 4H, β-pyrrole), 8.89 (s, 4H, β-pyrrole), 8.22–8.07 (m, 4H, ArH), 7.71–7.65 (m, 2H, ArH), 7.53–7.46 (m, 2H, ArH) 3.21–3.15 (m, 8H, TBA–CH_2), 1.41–1.33 (m, 10H, TBA–CH_3).

Compound 20:
Compound **20** was synthesized using a method similar to that reported by S. Ogi and co-workers.[8] Compound **19** (16.9 mg, 0.0120 mmol, 1.0 eq.), compound **12** (11.2 mg, 0.0306 mmol, 2.4 eq.), and Na_2CO_3 (6.73 mg, 0.0640 mmol, 5.0 eq.) were dissolved in anhydrous DMF (9 mL), EtOH (1 mL), and water (1 mL). The solution was deoxygenated through bubbling with N_2 at r.t. for 1 h. Tetrakis(triphenylphosphine)palladium(0) (1.5 mg, 0.0013 mmol, 0.03 eq.) was added and the resultant mixture was stirred at 110 °C for 4 h and then heated under reflux for 8 h under a N_2 atmosphere. The mixture was poured into aqueous $NaHCO_3$ (sat.) (5 mL) and extracted with CH_2Cl_2. The combined organic phases were dried (anhydrous Na_2SO_4). The residue was purified through column chromatography (CH_2Cl_2/MeOH/triethylamine, from 90/10/2 to 80/20/2) to yield a purple solid (39.8 mg, 95%).
^{1}H NMR (400 MHz, $CDCl_3$, TMS, r.t.) δ = 8.97–8.93 (m, 8H, β-pyrrole), 8.33 (t, *J* = 8.6 Hz, 4H, ArH), 8.18 (d, *J* = 8.6 Hz, 4H, ArH), 8.09 (d, *J* = 8.6 Hz, 4H, ArH), 7.27 (d, *J* = 8.6 Hz, 4H, ArH), 4.39 (t, *J* = 4.9 Hz, 4H, OCH_2), 4.01 (t, *J* = 4.9 Hz, 4H, OCH_2), 3.85–3.81 (m, 4H, OCH_2), 3.75–3.72 (m, 4H, OCH_2), 3.70–3.64 (m, 4H, OCH_2), 3.58–3.54 (m, 4H, OCH_2), 3.37 (s, 6H, OCH_3) 3.42–3.38 (m, 21H, TBA–CH_2), 1.55–1.43 (m, 27H, TBA–CH_3).

Compound 21:

Compound **20** (39.8 mg, 0.024 mmol, 1.0 eq.) was dissolved in CH_2Cl_2 (5 mL). Trifluoroacetic acid (100 μL) was added to the solution and the resultant mixture was stirred at r.t. for 1.5 h. The mixture was neutralized with triethylamine (500 μL) and then poured into water (5 mL) and extracted with CH_2Cl_2. The combined organic phases were dried (anhydrous Na_2SO_4) to yield a purple solid (8.0 mg, 47%).
^{1}H NMR (400 MHz, $CDCl_3$, TMS, r.t.) δ = 8.84–8.89 (m, 8H, β-pyrrole), 8.30–8.35 (m, 4H, ArH), 8.19–8.24 (m, 4H, ArH), 8.10 (d, *J* = 8.6 Hz, 4H, ArH), 7.30 (d, *J* = 8.6 Hz, 4H, ArH), 4.44 (t, *J* = 4.6 Hz, 4H, OCH_2), 4.07 (t, *J* = 4.9 Hz, 4H, OCH_2), 3.86–3.91 (m, 4H, OCH_2), 3.81–3.78 (m, 4H, OCH_2), 3.76–3.74 (m, 4H, OCH_2), 3.61–3.65 (m, 4H), 3.42 (s, 6H, OCH_3) –2.82 (s, 2H, pyrrole NH).

H_2TPPS_2-O-EG_2

Compound **21** was dissolved in distilled water and then the solution was passed through an ion exchange column (Amberlite® ion exchange resin; Na-form). After washing the aqueous solution with hexane and CH_2Cl_2, evaporation of the solvent under reduced pressure to yield a purple solid (10.5 mg, 99%).
^{1}H NMR (400 MHz, DMSO-d_6) δ 8.89–8.81 (m, 8H, β-pyrrole), 8.18 (d, *J* = 8.4 Hz, 4H, ArH), 8.14 (d, *J* = 8.4 Hz, 4H, ArH), 8.05 (d, *J* = 8.4 Hz, 4H, ArH), 7.40 (d, *J* = 9.2 Hz, 4H), 4.42 (t, *J* = 4.6 Hz, 4H), 3.94 (t, *J* = 4.6 Hz, 4H, OCH_2), 3.74–3.72 (m, 4H, OCH_2), 3.66–3.60 (m, 8H, OCH_2), 3.52–3.48 (m, 4H, OCH_2), 3.29 (s, 6H, OCH_3), –2.91 (s, 2H, pyrrole NH). ^{13}C NMR (100 MHz, DMSO-d_6) δ 158.5, 147.8, 141.5, 135.5, 133.8, 133.5, 131.7, 129.8, 124.3, 119.6, 120.0, 113.0, 71.9, 70.6, 70.4, 70.2, 69.6, 67.9, 58.6. MS (MALDI-TOF, negative mode, α-CHCA) *m*/*z* 1097.1 (calcd. for $[M - 2Na + H]^-$, 1097.3).

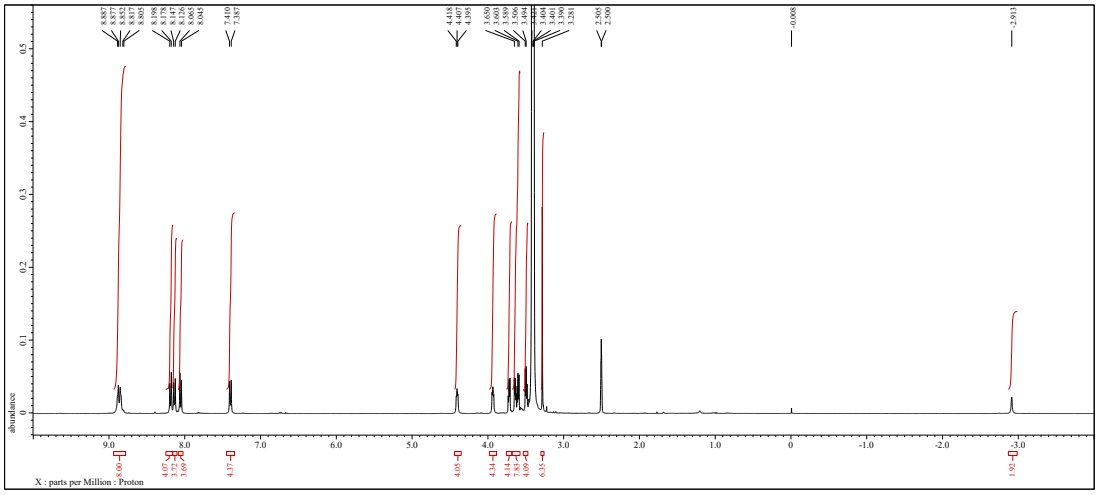

Fig. S13. ^{1}H NMR spectrum of **H_2TPPS$_2$-O-EG$_2$** in DMSO-d_6 at r.t.

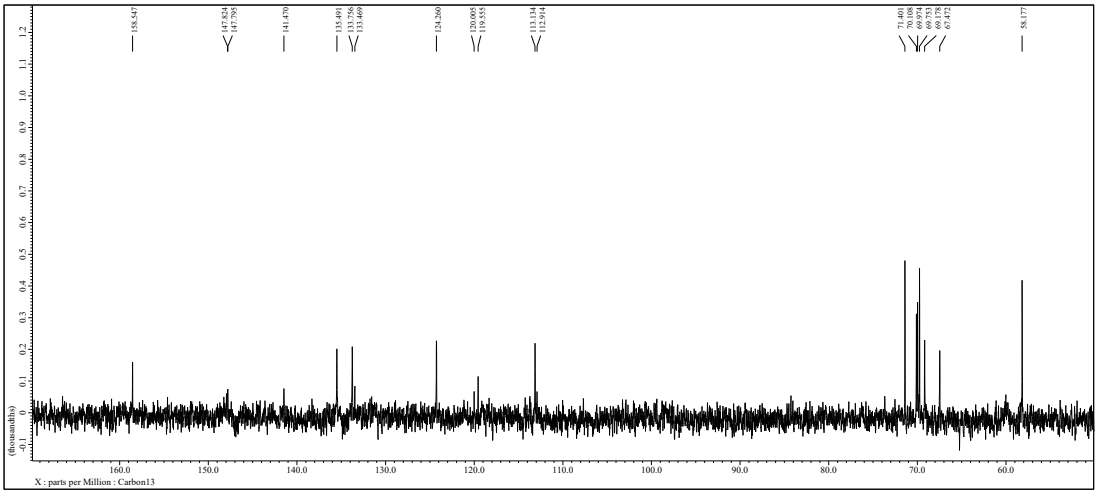

Fig. S14. ^{13}C NMR spectrum of **H_2TPPS$_2$-O-EG$_2$** in DMSO-d_6 at r.t.

Compound 22:

Compound **18** (48.4 mg, 0.038 mmol, 1.0 eq.), compound **15** (48.6 mg, 0.092 mmol, 2.4 eq.), and Na_2CO_3 (20.2 mg, 0.192 mmol, 5.0 eq.) were dissolved in anhydrous DMF (9 mL), EtOH (1 mL), and water (1 mL). The solution was deoxygenated through bubbling with N_2 at r.t. for 1 h. Tetrakis(triphenylphosphine)palladium(0) (2.2 mg, 0.0019 mmol, 0.1 eq.) was added and the resultant mixture was stirred at 110 °C for 11 h under a N_2

atmosphere. The mixture was poured into aqueous $NaHCO_3$ (sat.) (5 mL) and extracted with CH_2Cl_2. The combined organic phases were dried (anhydrous Na_2SO_4). The residue was purified through column chromatography (CH_2Cl_2/MeOH/triethylamine, from 90/10/2 to 80/20/2) to yield a purple solid (61.7 mg, 82%).
^{1}H NMR (400 MHz, $CDCl_3$, TMS, r.t.) δ = 8.91 (d, *J* = 4.0 Hz, 4H, β-pyrrole), 8.84 (d, *J* = 4.0 Hz, 4H, β-pyrrole), 8.33 (t, *J* = 7.9 Hz, 4H, ArH), 8.18 (d, *J* = 7.9 Hz, 4H, ArH), 7.41–7.38 (d, *J* = 8.6 Hz, 4H, ArH), 6.93 (t, *J* = 2.1 Hz, 4H, ArH), 4.29 (t, *J* = 4.9 Hz, 8H, OCH_2), 3.93 (t, *J* = 4.9 Hz, 8H, OCH_2), 3.78–3.74 (m, 8H, OCH_2), 3.70–3.67 (m, 8H, OCH_2), 3.63–3.61 (m, 8H, OCH_2), 3.51–3.47 (m, 8H, OCH_2), 3.31 (s, 12H, OCH_3), 3.18–3.11 (m, 13H, TBA-CH_2), 1.36–1.32 (m, 19H, TBA-CH_3), –2.88 (s, 2H, pyrrole NH).

H_2TPPS$_2$-O-EG$_4$

Compound **22** was dissolved in distilled water and then the solution was passed through an ion exchange column (Amberlite® ion exchange resin; Na-form). After washing the aqueous solution with hexane and CH_2Cl_2, evaporation of the solvent under reduced pressure to yield a purple solid (58.1 mg, 72%).
^{1}H NMR (400 MHz, DMSO-d_6) ^{1}H-NMR (400 MHz, DMSO-d6) δ 8.96 (d, *J* = 4.3 Hz, 4H, β-pyrrole), 8.85 (d, *J* = 4.3 Hz, 4H, β-pyrrole), 8.19 (d, *J* = 8.4 Hz, 4H, ArH), 8.08 (d, *J* = 8.4 Hz, 4H, ArH), 7.40 (s, 4H, ArH), 7.02 (s, 2H, ArH), 4.31-4.30 (m, 8H, OCH_2), 3.83-3.81 (m, 8H, OCH_2), 3.63-3.60 (m, 8H, OCH_2), 3.55-3.52 (m, 8H, OCH_2), 3.50–3.47 (m, 8H, OCH_2), 3.37–3.35 (m, 8H, OCH_2), 3.15 (s, 12H, OCH_3), –2.95 (s, 2H, pyrrole NH). ^{13}C NMR (100 MHz, DMSO-d_6) δ 158.7, 158,4, 158.3, 148.2, 143.6, 141.9, 134.2, 124.7, 120.3, 120.0, 119.3, 116.3, 114.7, 71.7, 70.5, 70.3, 70.0, 69.5, 68.1, 58.5. MS (MALDI-TOF, negative mode, α-CHCA) *m*/*z* 1377.4 (calcd. for $[M - 2Na + H]^-$, 1376.5).

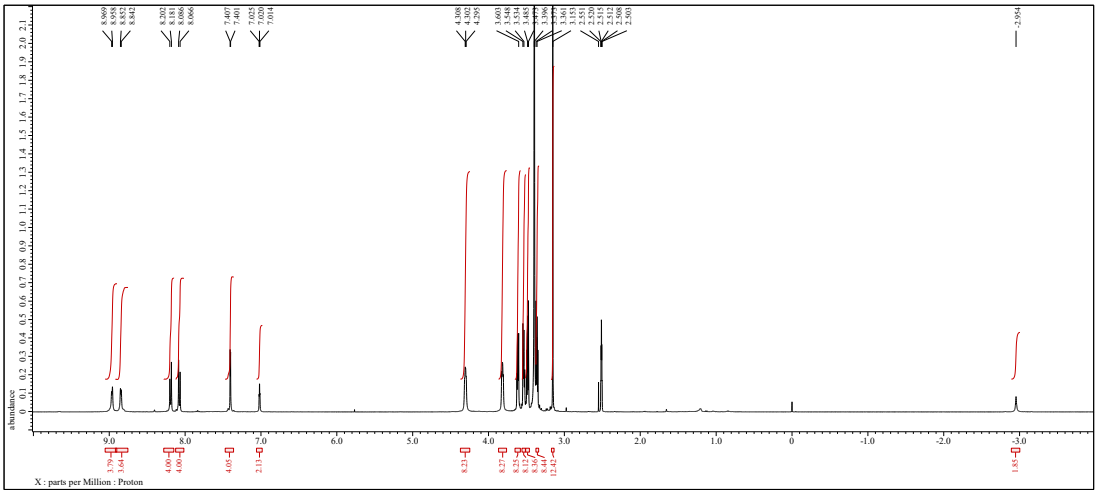

Fig. S15. ^{1}H NMR spectrum of **H_2TPPS_2-O-EG_4** in DMSO-d_6 at r.t.

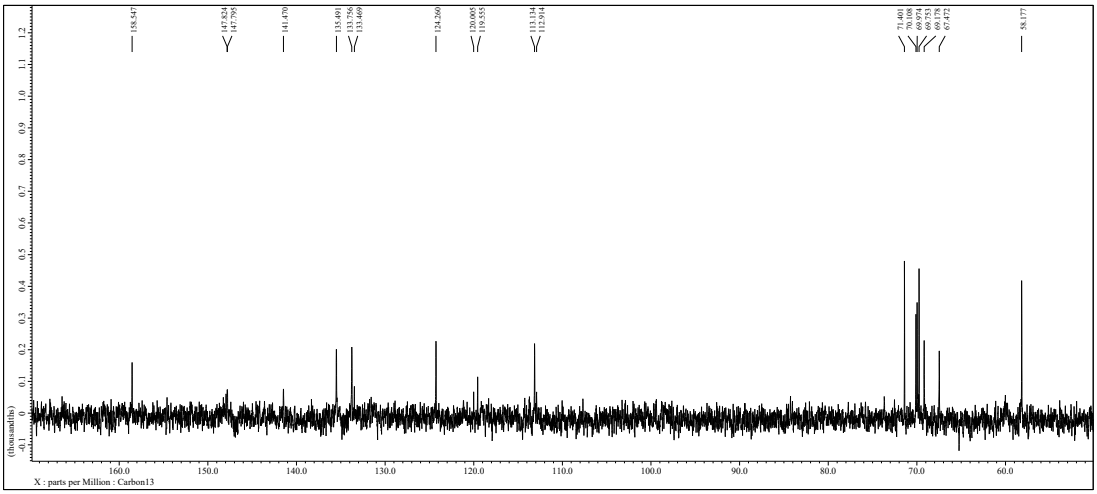

Fig. S16. ^{13}C NMR spectrum of **H_2TPPS_2-O-EG_4** in DMSO-d_6 at r.t.

5. Mass spectra of H_2TPPS_2-NHCO-EG_x (x = 2, 4, 6, 8, 18) and H_2TPPS_2-O-EG_x (x = 2, 4) porphyrin derivatives

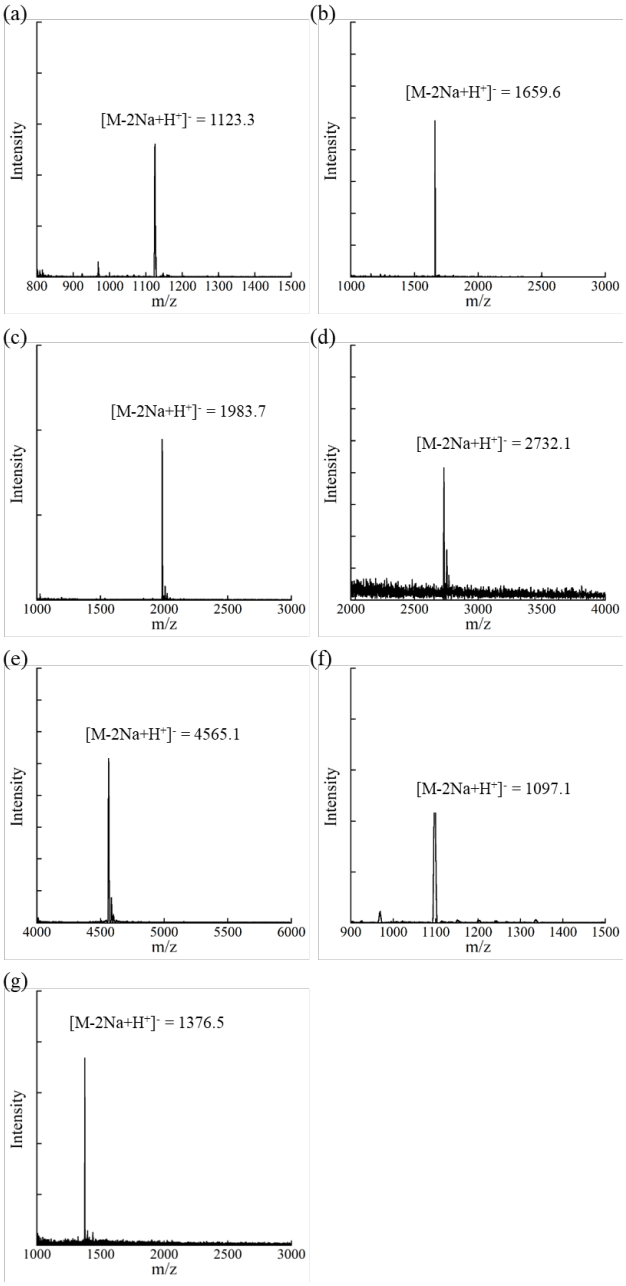

Fig. S17. Mass spectra of (a) H_2TPPS_2-NHCO-EG_2, (b) H_2TPPS_2-NHCO-EG_4, (c) H_2TPPS_2-NHCO-EG_6, (d) H_2TPPS_2-NHCO-EG_8, (e) H_2TPPS_2-NHCO-EG_{18}, (f) H_2TPPS_2-O-EG_2 and (g) H_2TPPS_2-O-EG_4 (MALDI-TOF, negative mode, α-CHCA).

6. Proton-triggered self-assembly of H_2TPPS_2-NHCO-EG_x (x = 2, 4, 6, 8, 18) in MeOH/water

6-1. DFT-calculated structures

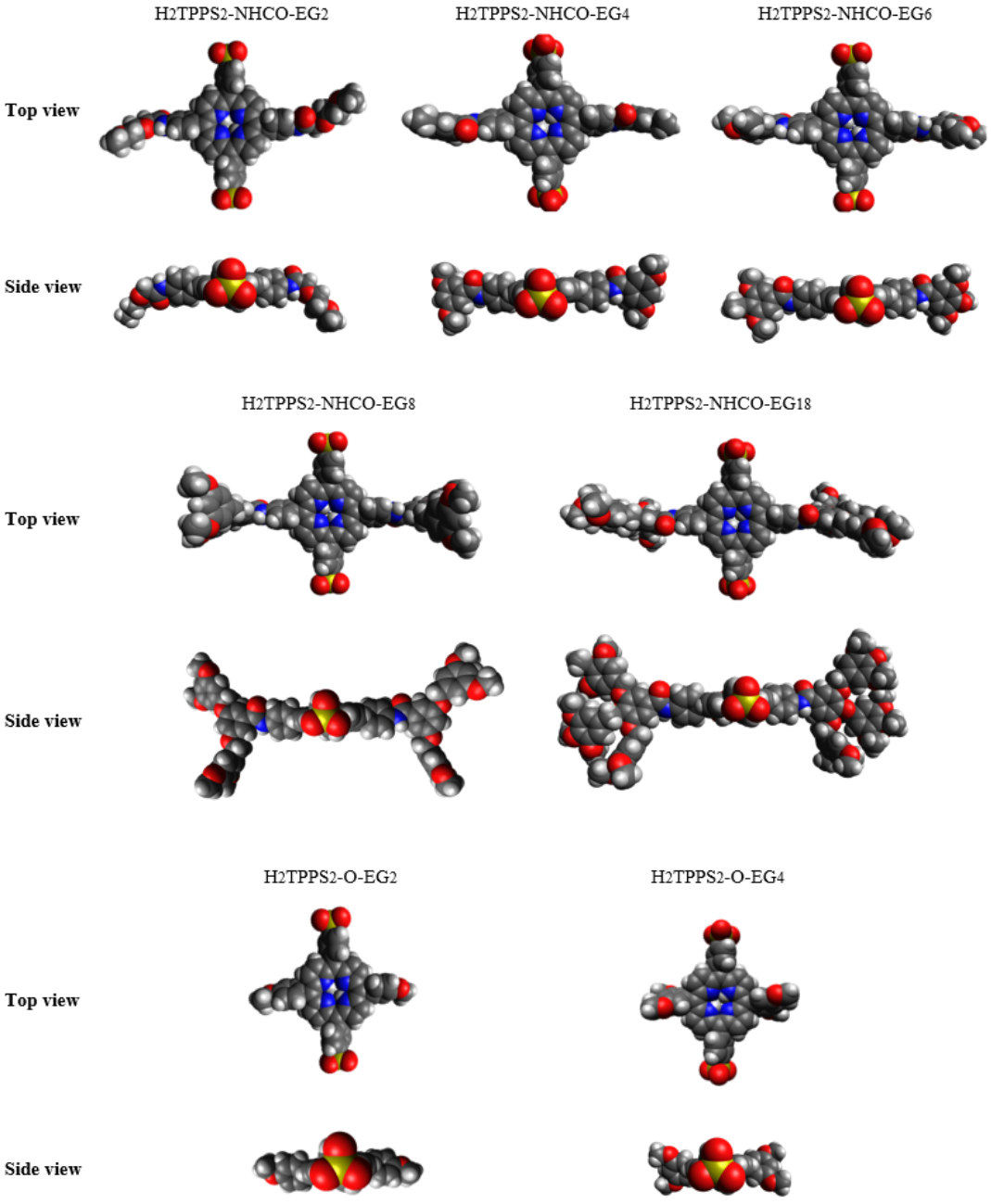

Fig. S18. DFT-calculated (at the B3LYP/6-31G+** level) structures of H_2TPPS_2-NHCO-EG_x derivatives (x = 2, 4, 6, 8, 18); for simplicity, the EG units have been replaced by CH_3 groups.

6-2. Solvent-dependent UV–Vis spectra

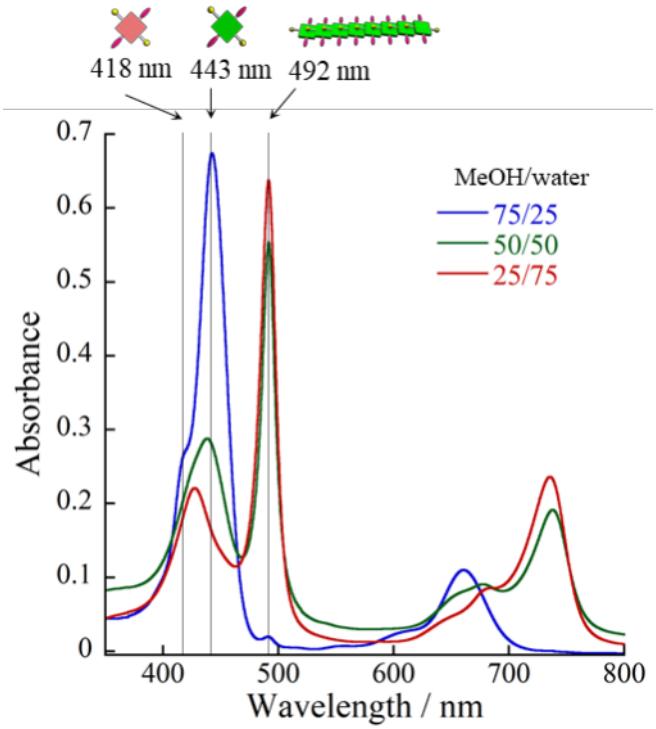

Fig. S19. Solvent-dependent UV–Vis spectra of H_2TPPS_2-NHCO-EG_2 in MeOH/aqueous HCl (pH 3) mixtures (25 μM; optical path length, 1 mm; r.t.): 75/25 (blue line), 50/50 (green line), and 25/75 (red line).

6-3. UV–Vis spectra of H_2TPPS_4 upon addition of aqueous HCl and AFM images of the resultant J-aggregate fibers

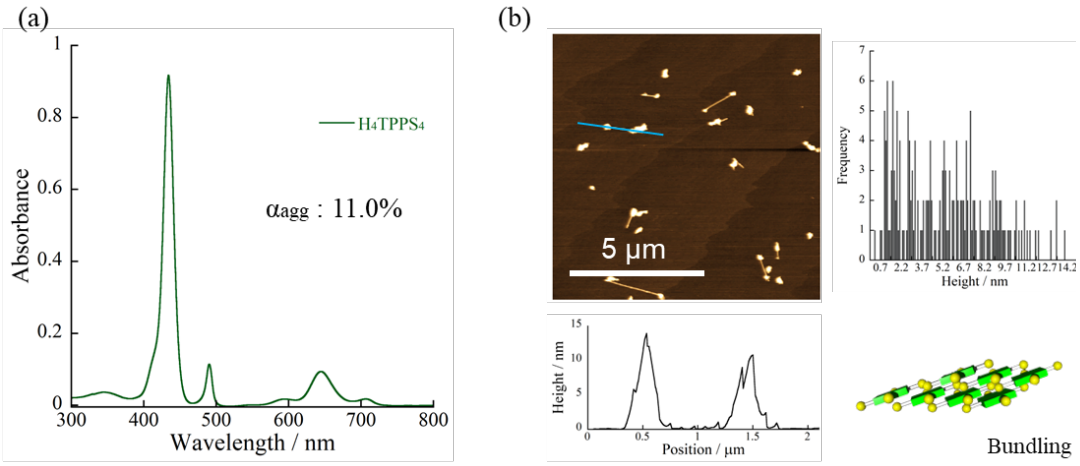

Fig. S20. (a) UV–Vis spectra of H_4TPPS_4 [25 μM in HCl (pH 3); optical path length, 1 mm; r.t]. (b) AFM image, height profile and height distribution of J-aggregate fibers [25 μM, in HCl (pH 3); mica substrate]. Height distribution was measured from AFM images of at least 100 fibers.

6-4. AFM images of J- and H-aggregates

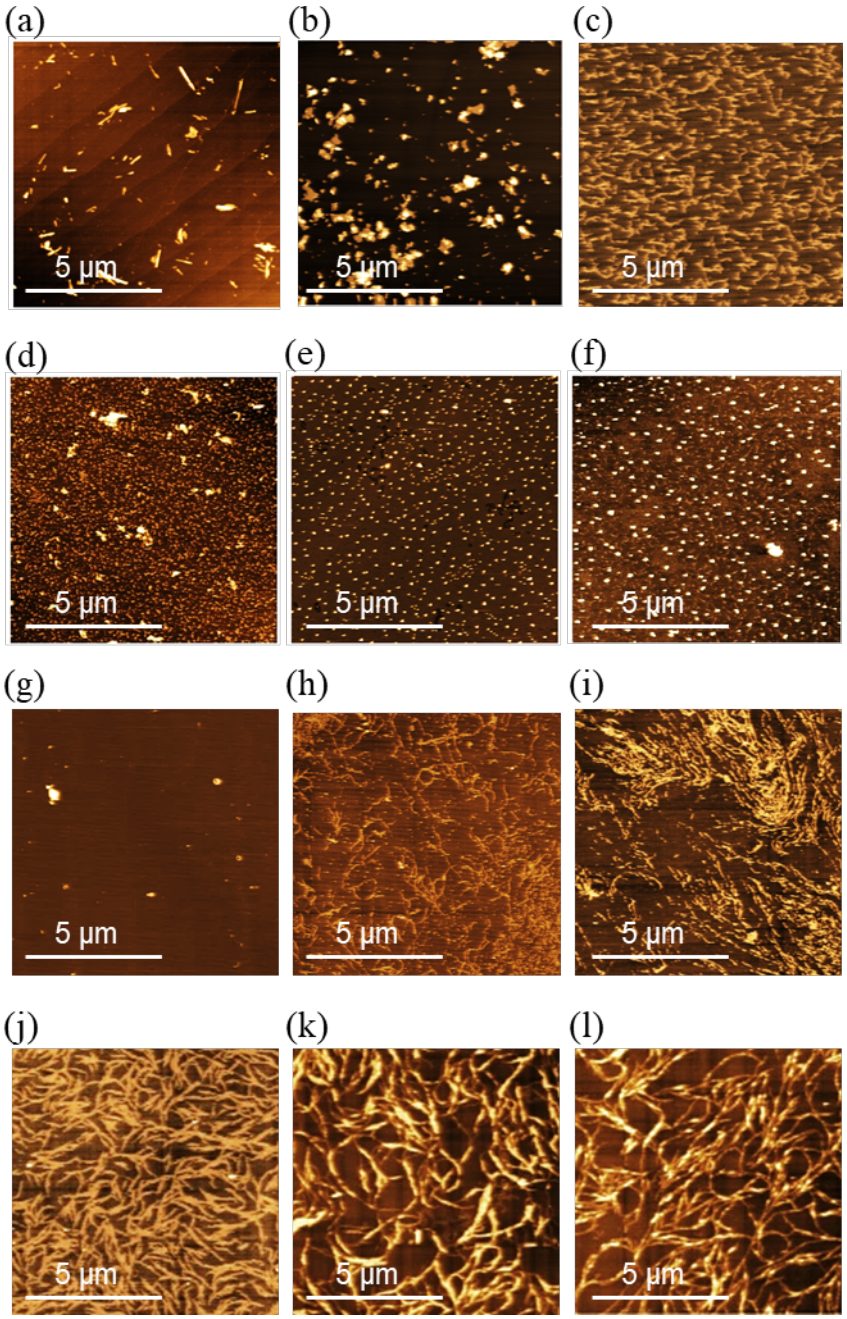

Fig. S21. (a–f) AFM images of (a) the J-aggregate nanofibers of H_4TPPS_2-NHCO-EG_2, (b) the sheet-like structures observed after standing the solution in (a) for 24 h, and (c–f) the aggregate structures of (c) H_4TPPS_2-NHCO-EG_4, (d) H_4TPPS_2-NHCO-EG_6, (e) H_4TPPS_2-NHCO-EG_8, and (f) H_4TPPS_2-NHCO-EG_{18} [25 μM, MeOH/aqueous HCl (pH 3), 25/75, 10 × 10 μm frame; mica substrate]. (g–l) AFM images of the H-aggregates formed form H_4TPPS_2-NHCO-EG_2 in MeOH/water mixtures: (g) MeOH/water = 50/50, (h) 40/60, (i) 30/70, (j) 25/75, (k) 10/90, and (l) 5/95 (25 μM; mica substrate).

6-5. SEM images of sheet structures

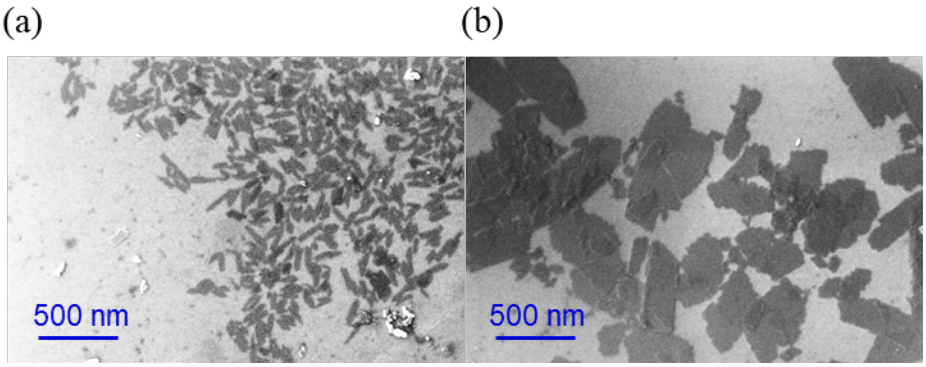

Fig. S22. SEM images of J-aggregate sheets formed from H_4TPPS_2-NHCO-EG_2 in MeOH/aqueous HCl (pH 3, 25/75) after standing the solution for (a) 1 and (b) 6 h.

6-6. Analysis of kinetic data obtained for J-aggregate formation in MeOH/aqueous HCl

According to the model suggested by R. F. Pasternack and co-workers, we employed a kinetic model for a system in which the assemblies catalyze the rate-limiting step in the aggregation process.[9] In these cases, the experimental rate constant is itself time-dependent. The expression for this model is

$$([\mathrm{M}] - [\mathrm{M}]_\infty)/([\mathrm{M}]_\mathrm{o} - [\mathrm{M}]_\infty) = (1 + (m - 1)\{k_0 t + (n + 1)^{-1}(k_\mathrm{c} t)^{\mathrm{n}+1}\})^{-1/(\mathrm{m}-1)} \quad \text{(Eq.1)}$$

where [M] is the free monomer concentration at time t; $[\mathrm{M}]_0$ is the initial total concentration of monomer units; $[\mathrm{M}]_\infty$ is the concentration of free monomer units at equilibrium; k_0 is the rate constant for the uncatalyzed growth; k_c is the rate constant for the catalytic pathway; n is a parameter that describes the growth of the chromophore assembly as a power function of time; and m ($\neq 1$) is related to the size of the "critical nucleus," the formation of which is the rate-determining step in the process. We set

$$([\mathrm{M}] - [\mathrm{M}]_\infty)/([\mathrm{M}]_0 - [\mathrm{M}]_\infty) = (\mathrm{Abs} - \mathrm{Abs}_\infty)/(\mathrm{Abs}_0 - \mathrm{Abs}_\infty)$$

where Abs is the absorbance of the solution at 492 nm.

Fig. S23 presents the fits of the kinetic data to this autocatalytic model for the aggregation processes of H_2TPPS_2-NHCO-EG_2 and H_2TPPS_2-NHCO-EG_4.

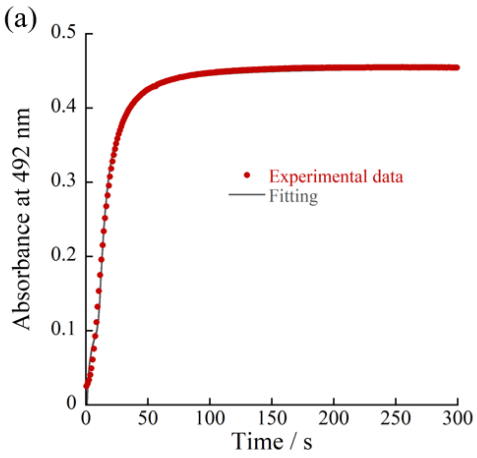

k_0 / s^{-1}	0.710
k_c / s^{-1}	0.128
m	10.6
n	14.2

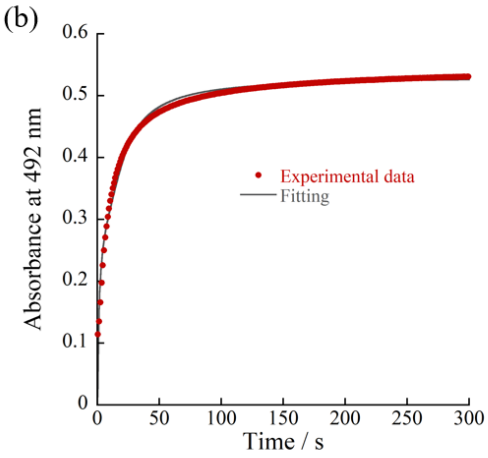

k_0 / s^{-1}	1.11
k_c / s^{-1}	0.16
m	4.73
n	3.69

Fig. S23. Time-dependent absorbance data at 492 nm (assignable to J-aggregates; red circles) and the fits (continuous lines) to Eq. 1 of (a) H_4TPPS_2-NHCO-EG_2 and (b) H_4TPPS_2-NHCO-EG_4 (5 μM; optical path length, 3 mm; MeOH/aqueous HCl (pH 3), 25/75). (a, b) Tables providing kinetic parameters for the self-assembly of (a) H_4TPPS_2-NHCO-EG_2 and (b) H_4TPPS_2-NHCO-EG_4.

6-7. Time-dependent IR spectral changes upon formation of sheet structure

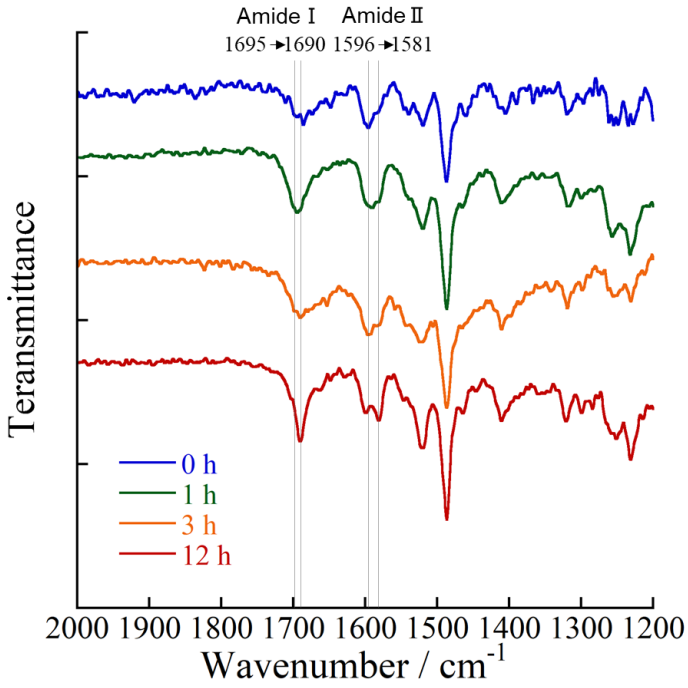

Fig. S24. Time-dependent IR spectra upon formation of sheet structures. Each solution was cast onto a CaF_2 substrate and dried under reduced pressure prior to observation. Amide I and II band regions in the IR spectra of the J-aggregates prepared in MeOH/aqueous HCl (pH 3), 25/75. We began recording spectra immediately after addition of aqueous HCl to a solution of H_2TPPS_2-NHCO-EG_2 (0 h). After standing the solutions for 1, 3, and 12 h, each solution was cast onto a substrate and subjected to the spectral measurements.

6-8. Estimation of absorption maxima of oligomers of H_4TPPS_2-NHCO-EG_6

In general, during cooperative polymerization processes, the oligomeric intermediates are not detectable, due to very rapid elongation. For example, in a previous paper [10], describing *in situ* dynamic analysis of supramolecular polymerization using microflow channel, we found that the rate of self-assembly of the parent H_2TPPS_4 was typically on the order of milliseconds. Here, the ability to observe absorption bands corresponding to oligomers in steady-state UV–Vis spectra implies that the very rapid elongation rates arising from strong interactions between the porphyrin derivatives had been moderated, balanced by the steric bulk of the peripheral EG_6 units.

According to the model suggested by J. M. Ribo and co-workers, we calculated the interaction energy (E_n) from[11]

$$E_n = E_\infty \cos\left(\frac{\pi}{N+1}\right) \qquad \text{(Eq. 2)}$$

where N is the length and E_∞ is the energy of the infinite extended interaction, equal to the energy difference between the monomer (431 nm) and J-aggregate (493 nm).

(a)

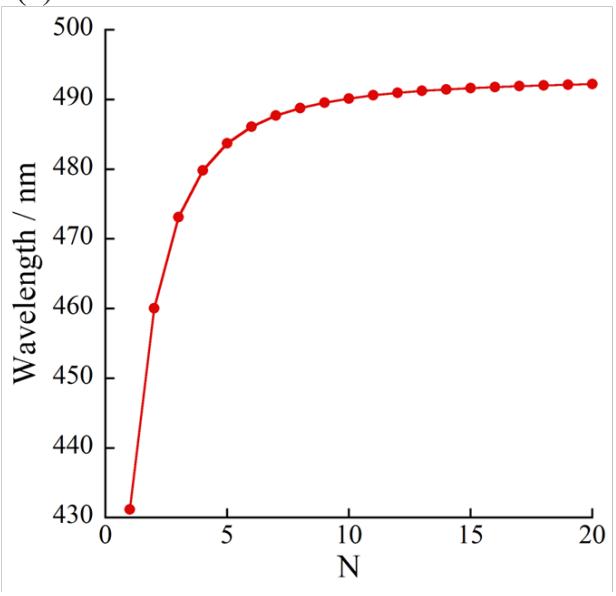

(b)

N	Wavelength / nm
1(monomer)	431.2
2	460.0
3	473.1
4	479.9
5	483.7
6	486.1
7	487.7
8	488.8
9	489.6
10	490.2
11	490.6
12	491.0
13	491.2
14	491.5
15	491.7
16	491.8
17	491.9
18	492.0
19	492.1
20	492.2
∞ (J-aggregate)	493.0

Fig. S25. Expected wavelengths for the J-aggregate bands of the oligomers of H_4TPPS_2-NHCO-EG_6.

6-9. Deconvoluted UV–Vis spectra of J-aggregated supramolecular polymers (oligomers) of H_4TPPS_2-NHCO-EG_6

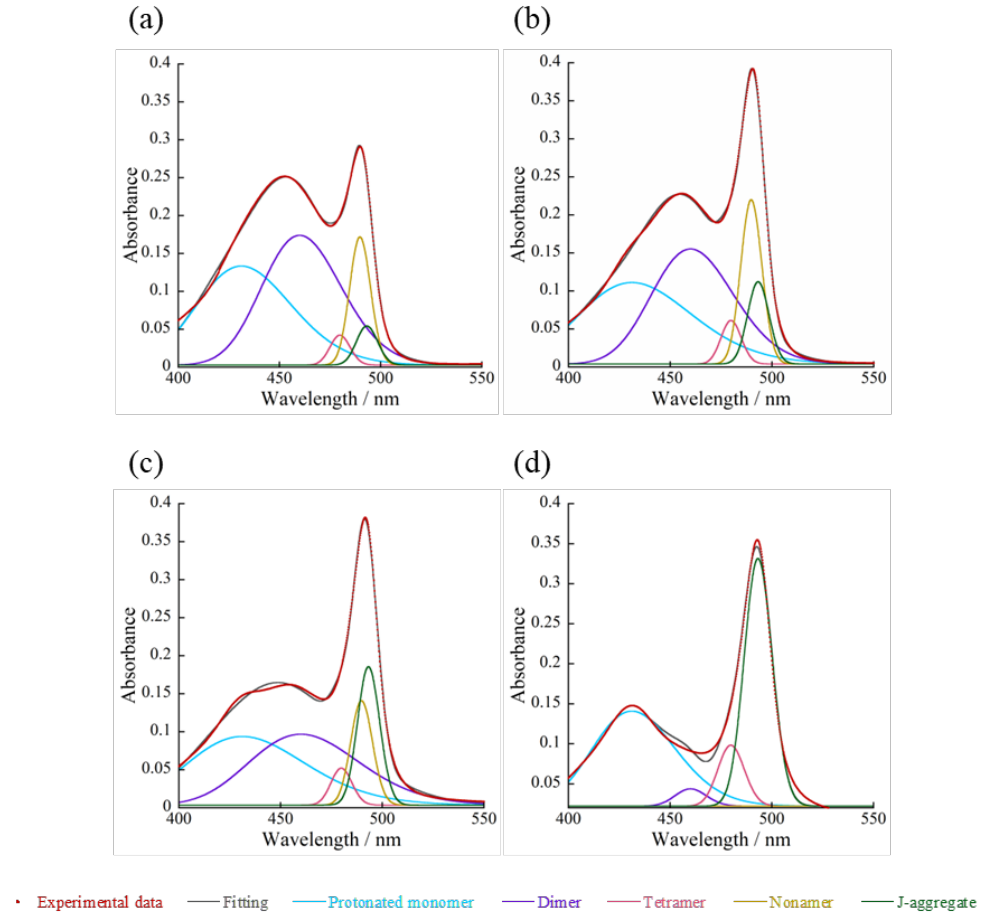

Fig. S26. Deconvoluted UV–Vis spectra of J-aggregated supramolecular polymers (oligomers) formed from H_4TPPS_2-NHCO-EG_6, recorded (a) 0, (b) 1, (c) 30, and (d) 100 min after mixing with aqueous HCl (final solvent composition: MeOH/aqueous HCl, 25/75; final pH, 3; 25 μM; optical path length, 1 mm; r.t.).

7. Self-assembly of H_2TPPS_2-NHCO-EG_x (x = 2, 4, 6, 8, 18) in DMF/water

Because the parent H_2TPPS_2 is soluble in DMF, to directly compare the self-assembly of H_2TPPS_2-NHCO-EG_x with H_2TPPS_2 we investigated the behavior of H_2TPPS_2-NHCO-EG_x in DMF/aqueous HCl. Throughout these experiments, the final concentration was fixed at 25 µM and the solvent composition was DMF/water, 2/98. The final pH was adjusted in the range from 3.0 to 2.0.

7-1. UV–Vis spectra of H_4TPPS_2-NHCO-EG_x (x = 2, 4, 6, 8, and 18) in DMF/water (pH = 2)

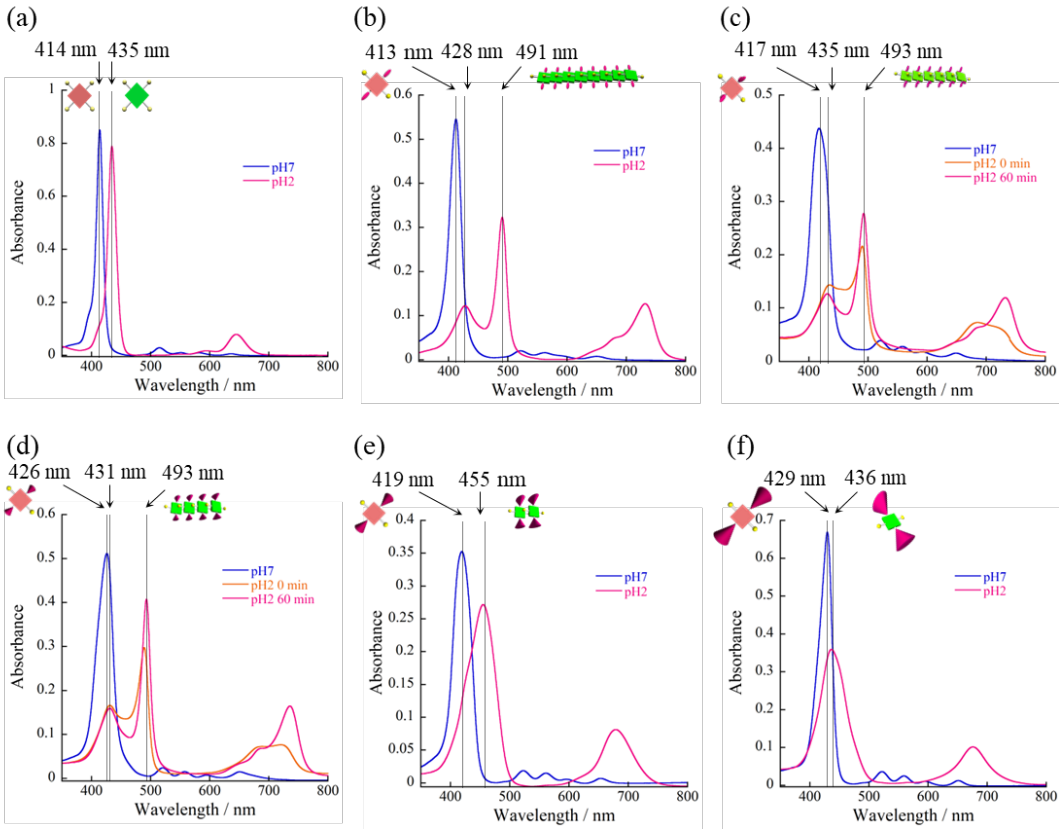

Fig. S27. UV–Vis spectra of (a) H_2TPPS_4, (b) H_2TPPS_2-NHCO-EG_2, (c) H_2TPPS_2-NHCO-EG_4, (d) H_2TPPS_2-NHCO-EG_6, (e) H_2TPPS_2-NHCO-EG_8, and (f) H_2TPPS_2-NHCO-EG_{18} (25 µM; optical path length, 1 mm; r.t.). Blue lines are the spectra recorded in DMF/water = 2/98 (pH 7). Orange and magenta lines are the spectra recorded in DMF/aqueous HCl, 2/98 (pH 2). Orange lines in (c) and (d) are the spectra recorded immediately after addition of aqueous HCl (0 min); the magenta lines are the spectra obtained after 60 min.

8. Attempted face-to-face stacking of anionic H_2TPPS_2-NHCO-EG_x (x = 2, 4, 6, 8, and 18) in MeOH/water

8-1. Deconvoluted UV–Vis spectra of H-aggregated supramolecular polymers of H_2TPPS_2-NHCO-EG_2

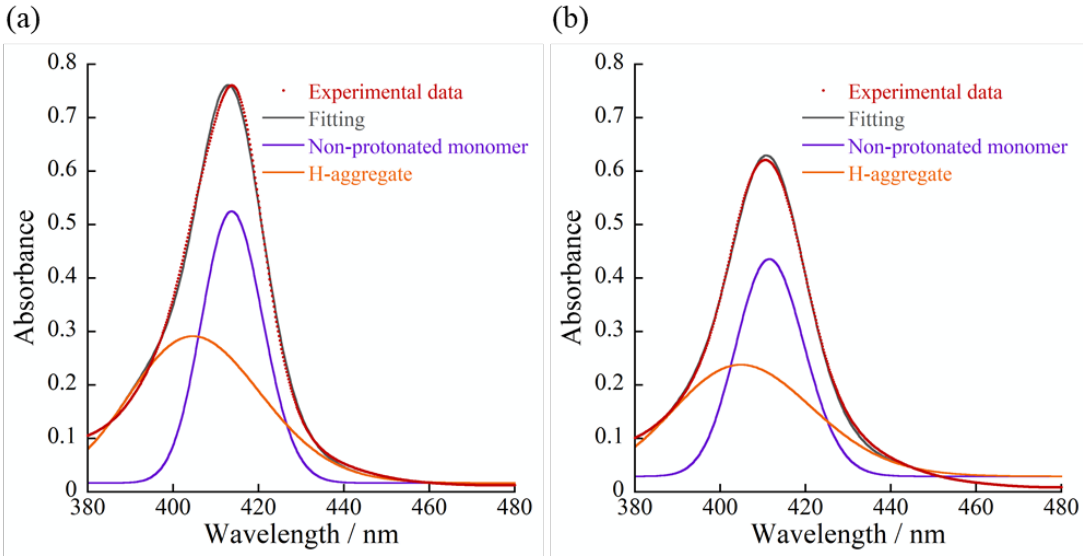

Fig. S28. Deconvoluted UV–Vis spectra of H-aggregated supramolecular polymers formed from H_2TPPS_2-NHCO-EG_2 in MeOH/water mixtures: (a) 25/75 and (b) 5/95 (25 μM; optical path length, 1 mm; r.t.).

From these deconvoluted spectra, the blue-shifted peak at 405 nm that appeared upon addition of water can be reasonably assigned to the H-aggregate. Although the absorption intensity at 415 nm continued to decrease upon increasing the water content (MeOH/water) from 25/75 to 5/95, the intensity at 405 nm did not change any further. This situation arose, presumably, because at this stage the increase in the absorption at 405 nm, due to the blue-shift, was (coincidently) cancelled out by the hypsochromic effect of the whole spectrum.

8-2. Temperature-dependent study and analysis of H-aggregated supramolecular polymers

A solution of H_2TPPS_2-NHCO-EG_2 in MeOH/aqueous HCl (pH 3) = 25/75 (25 μM) was prepared following the protocol mentioned above (Section 2) and heated by a Peltier device at 343 K for 15 min. The solution was cooled and the absorption at a single wavelength (405 nm) was monitored as function of temperature (from 343 to 278 K at 1 K min^{-1}).

The degree of aggregation (α) was calculated from[12]

$$\alpha(T) = \frac{\varepsilon(T)-\varepsilon_{MIN}}{\varepsilon_{MAX}-\varepsilon_{MIN}} \quad \text{(Eq. 3)}$$

where $\varepsilon(T)$ is the measured extinction coefficient at temperature T and ε_{MAX} and ε_{MIN} are the maximum and minimum extinction coefficients, respectively.

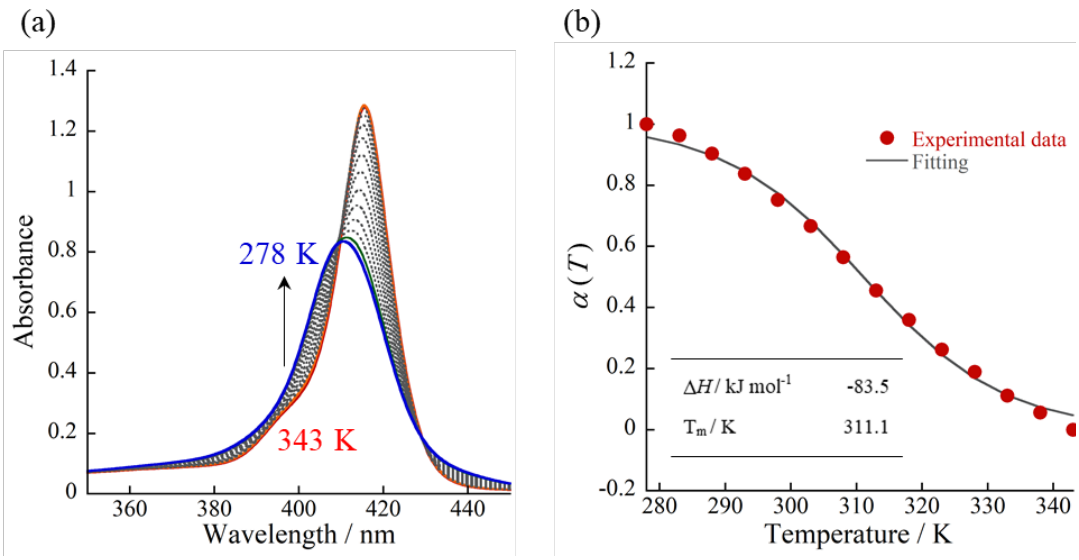

Fig. S29. Temperature-dependent aggregation behavior for H_2TPPS_2-NHCO-EG_2 (25 μM; optical path length, 1 mm; MeOH/water, 25/75): (a) UV–Vis spectra and (b) plot of the degree of aggregation (α) based on the absorbance at 405 nm (assignable to H-aggregates; red circles) and data fitted (continuous line) to an isodesmic supramolecular polymerization model. Inset: Thermodynamic parameters for the self-assembly of H_2TPPS_2-NHCO-EG_2, evaluated by fitting an isodesmic supramolecular polymerization model. T_m is the melting temperature (α = 0.5 at $T = T_m$); ΔH is the molecular enthalpy released during elongation.

9. Self-assembly of H_2TPPS_2-O-EG_x (x = 2, 4) in MeOH/water

9-1. Deconvoluted UV–Vis spectra of H-aggregated supramolecular polymers of H_2TPPS_2-O-EG_2

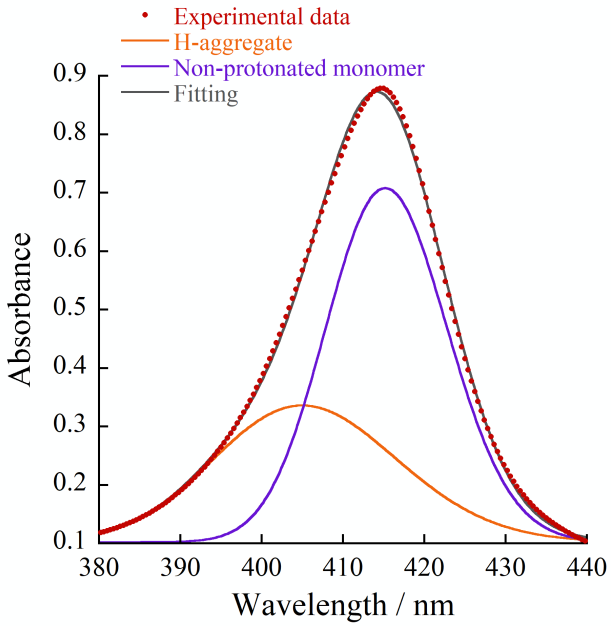

Fig. S30. Deconvoluted UV–Vis spectra of H-aggregated nanofibers formed from H_2TPPS_2-O-EG_2 in MeOH/water = 25/75 (25 μM; optical path length, 1 mm; r.t.).

9-2. Temperature-dependent study and analysis of H-aggregated supramolecular polymers of H_2TPPS_2-O-EG_2

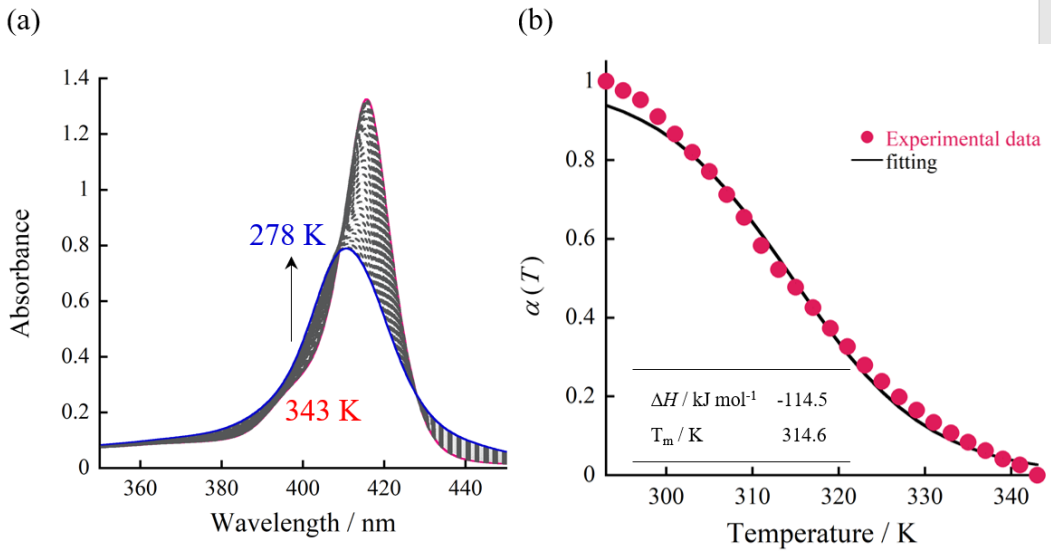

Fig. S31. Temperature-dependent aggregation behavior for H_2TPPS_2-O-EG_2 in the presence of NaCl (25 μM; optical path length, 1 mm; MeOH/water, 25/75): (a) UV–Vis spectra and (b) plot of the degree of aggregation (α) based on the absorbance at 405 nm (assignable to H-aggregates; red circles) and data fitted (continuous line) to an isodesmic supramolecular polymerization model. Inset: Thermodynamic parameters for the self-assembly of H_2TPPS_2-O-EG_2, evaluated by fitting an isodesmic supramolecular polymerization model. T_m is the melting temperature ($\alpha = 0.5$ at $T = T_m$); ΔH is the molecular enthalpy released during elongation.

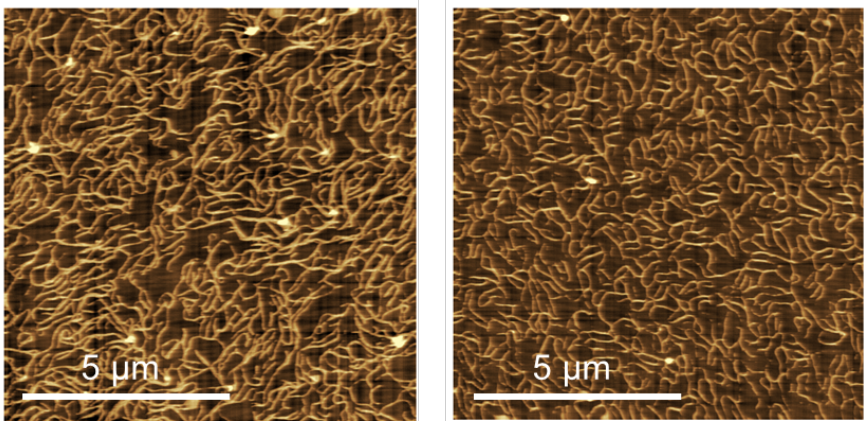

Fig. S32. AFM images of H-aggregate of H_2TPPS_2-O-EG_2 prepared in the presence of excess NaCl (mica substrate).

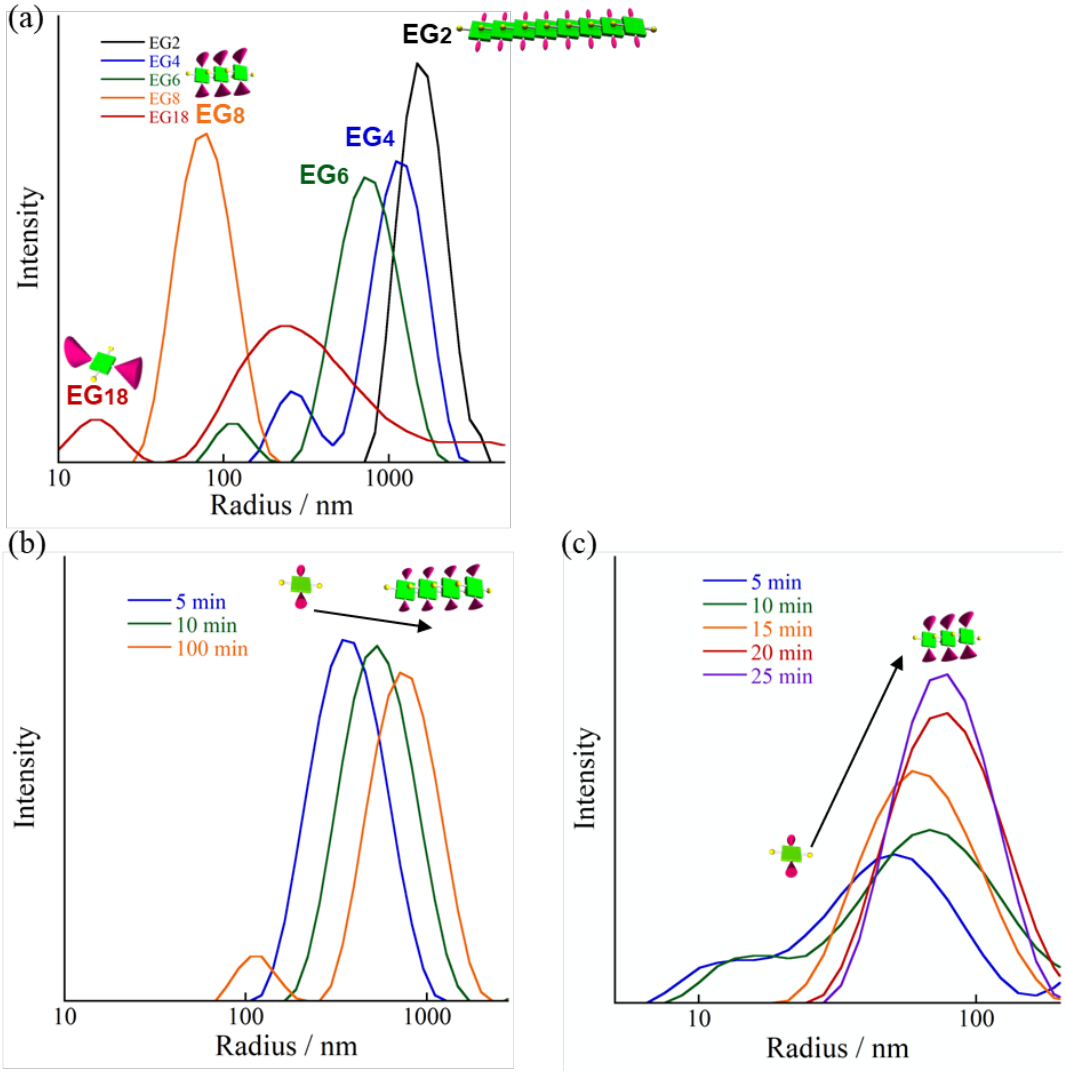

Fig. S33. (a) DLS data of J-aggregate species of H_2TPPS_2-NHCO-EG_x derivatives (x = 2, 4, 6, 8, 18) in MeOH/water (for H_2TPPS_2-NHCO-EG_6 and H_2TPPS_2-NHCO-EG_8, data was recorded at 100 and 25 min after mixing with aqueous HCl, respectively. Time-dependent changes in the hydrodynamic radius of (b) H_2TPPS_2-NHCO-EG_6 and (c) H_2TPPS_2-NHCO-EG_8.

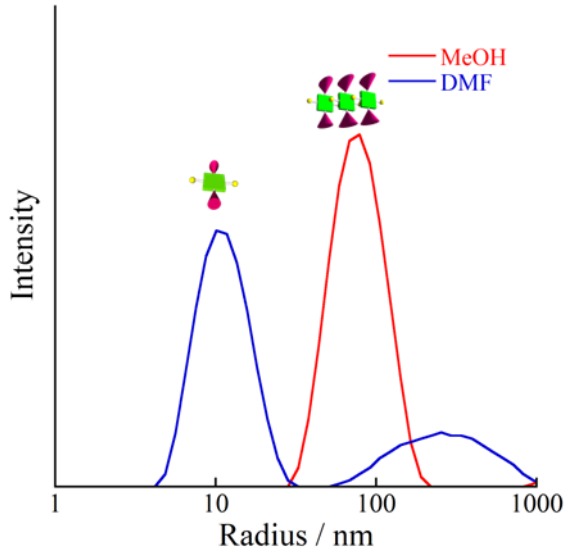

Fig. S34. DLS data of H_2TPPS_2-NHCO-EG_8 J-aggregates prepared in MeOH/water (redline) and in DMF/water (blue line).

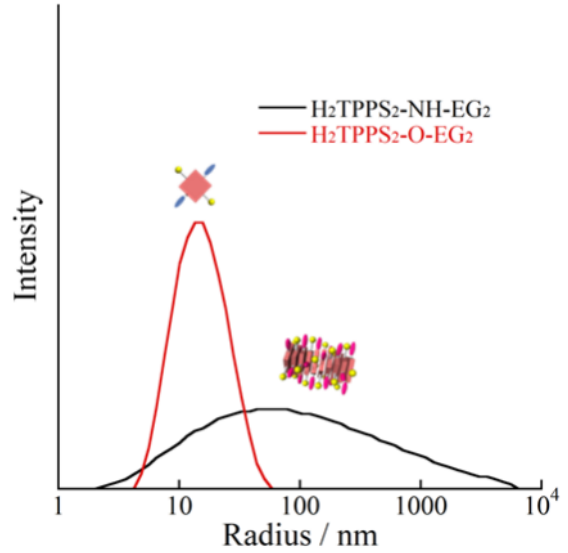

Fig. S35. DLS data of H-aggregate of H_2TPPS_2-NHCO-EG_2 (black line) and H_2TPPS_2-O-EG_2 (red line) in MeOH/water.

10. References

1. T. Lin, X. S. Shang, J. Adisoejoso, P. N. Liu and N. Lin, *J. Am. Chem. Soc.,* 2013, **135**, 3576-3582.
2. A. Arlegui, Z. El-Hachemi, J. Crusats and A. Moyano, *Molecules*, 2018, **23**, 3363.
3. V. Percec, D. A. Wilson, P. Leowanawat, C. J. Wilson, A. D. Hughes, M. S. Kaucher, D. A. Hammer, D. H. Levine, A. J. Kim, F. S. Bates, K. P. Davis, T. P. Lodge, M. L. Klein, R. H. DeVane, E. Aqad, B. M. Rosen, A. O. Argintaru, M. J. Sienkowska, K. Rissanen, S. Nummelin and J. Ropponen, *Science*, 2010, **328**, 1009-1014.
4. A. Bertin, J. Steibel, A. I. Michou-Gallani, J. L. Gallani and D. Felder-Flesch, *Bioconjugate Chem.*, 2009, **20**, 760-767.
5. H. Kitagishi, H. Kawasaki and K. Kano, *Chem. Asian. J.*, 2015, **10**, 1768-1775.
6. V. Bloemendal, D. Sondag, H. Elferink, T. J. Boltje, J. C. M. van Hest and F. Rutjes, *Eur. J. Org. Chem.*, 2019, **2019**, 2289-2296.
7. X. Jiang, F. Gou and H. Jing, *J. Catal.*, 2014, **313**, 159-167.
8. S. Ogi, K. Sugiyasu, S. Manna, S. Samitsu and M. Takeuchi, *Nat. Chem.*, 2014, **6**, 188-195.
9. R. F. Pasternack, C. Fleming, S. Herring, P. J. Collings, J. dePaula, G. DeCastro and E. J. Gibbs, *Biophys. J.*, 2000, **79**, 550-560.
10. C. Kanzaki, A. Inagawa, G. Fukuhara, T. Okada and M. Numata, *ChemSystemsChem*, 2020, **2**, e2000006.
11. A. Sorrenti, Z. El-Hachemi, J. Crusats and J. M. Ribo, *Chem. Commun.*, 2011, **47**, 8551-8553.
12. M. M. Smulders, M. M. Nieuwenhuizen, T. F. de Greef, P. van der Schoot, A. P. Schenning and E. W. Meijer, *Chem. Eur. J.*, 2010, **16**, 362-367.